Effects of Ultrasound and Microwaves on selective Reduction: Catalyst Preparation and Reactions

(Article begins on next page)

20 August 2022

Effects of Ultrasound and Microwaves on Selective Reduction: Catalyst Preparation and Reactions

Zhilin Wu,[a] Emily Borretto,[a] Jonathan Medlock,[b] Werner Bonrath[b] and Giancarlo Cravotto*[a]
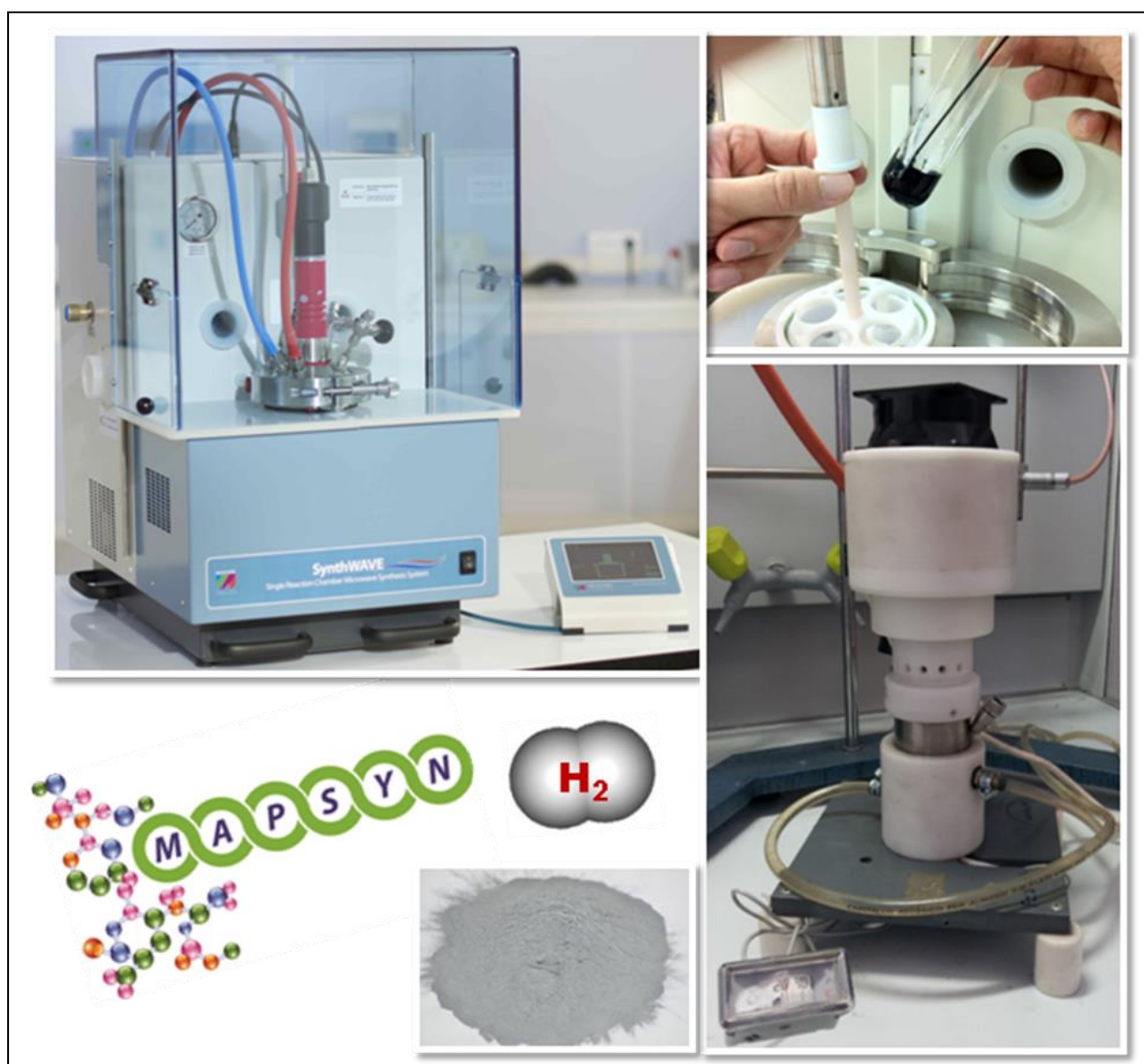
The reduction of organic compounds via catalytic hydrogenation is an important transformation in organic chemistry, especially in the synthesis of fine chemicals, natural products and pharmaceuticals. This review mainly focuses on the selective reduction of substrates with multiple functional groups. Literature from the last two decades has proved the pivotal role that ultrasound and microwaves can play not only in the preparation of environmentally friendly, efficient catalysts but also in their use in catalytic reactions. Due to the specific selective activation of the solid catalyst surface, dielectric heating and acoustic cavitation may dramatically enhance the reaction rate and selectivity. A thorough literature survey was the first step in the MAPSYN project (EU 7th Framework Program) and has the goal of the industrial demonstration of selective hydrogenations intensified by microwaves and ultrasound. Both techniques are irreplaceable tools in heterogeneous catalysis and can be expected to bring even greater successes in the near future as processes are scaled up with suitable flow-reactors equipped with on-line analytical monitoring.

Introduction

More than 80% of all chemical and pharmaceutical production processes (worth ~ €1500 billion), depend on catalytic technologies. Catalysis directly contributes about 3% of the EU's Gross Domestic Product (GDP), a value that grows 10 times if one takes into account industries that depend on chemical raw materials. Catalysis innovation is therefore decisive in tapping new feedstocks, producing high performance materials and creating environment-friendly processes.[1,2] Chemical industries are heavily involved in the development of mild, simple, environmental friendly and inexpensive catalytic processes that respect the principles of green chemistry. Supported catalysts are key systems in sustainable chemical processes because they are readily reused and recycled, and generally have low toxicity.[3,4] Metal nanoparticles based heterogeneous catalysts have been widely investigated, due to their high activity. Nano-scale metal colloids and clusters have unique physical and chemical properties,[5] which are absent in the bulk phase, and find very important applications in many fields of academic and industrial interest, in particular heterogeneous catalysis.[6] Therefore, non-conventional enabling technologies such as ultrasound (US) and microwaves (MW) foster process intensification and combine safer protocols, cost reduction and energy savings.[7] The excellent results on catalyst preparation by means of US- or MW-assisted protocols reported in the literature may open the way for larger-scale work which may see the use of loop reactors with multiple units combined in a sequential manner.[8,9]

Selective or partial catalytic reduction is widely applied in the synthesis of intermediates of pesticides, herbicides, drugs, pigments and dyes. Since the early 1980s, US has been applied for the activation of heterogeneous catalytic hydrogenations.[10-14] US is one of the promising techniques in green organic and pharmaceutical synthesis as well as in chemical process intensification. This innovation was devised to create more compact, safer, energy efficient and environmentally friendly processes.[15-18] Essentially, US has no direct action on chemical bonds, however, the significant enhancement in selectivity, rates and yields under mild reaction conditions in both homogeneous and heterogeneous systems has been achieved by means of sonication (the act of applying US energy),[17-19] which can even increase reactivity almost a million-fold.[20]

[a] Dr. Z. Wu, Dr. E. Borretto, Prof. G. Cravotto
Dipartimento di Scienza e Tecnologia del Farmaco, and
Interdepartmental Centre "Nanostructured interfaces and surfaces-
NIS, University of Turin, via Pietro Giuria 9, 10125 Turin
Fax: (+39)0116707687
E-mail: giancarlo.cravotto@unito.it
[b] Dr. J. Medlock, Dr. W. Bonrath
DSM Nutritional Products Ltd., Research and Development
P.O. Box 2676, 4002 Basel, Switzerland.

The chemical and physical effects of US arise from cavitation phenomenon which produces localized extreme conditions (short-lived hot spots). Sonication can improve yields and selectivity, generate reactive species, active catalyst surfaces and enable the replacement of hazardous reagents. US enables the rapid dispersion of solids and allows the formation of porous materials and nanostructures.[18] Sonication can also inhibit particle aggregation thanks to the intense implosion of acoustic cavitation.[21-24] The US-assisted chemical reduction method has been successfully applied in the preparation of amorphous alloys with homogeneous particle size.[25] When a cavitation bubble violently collapses near a solid surface, the high-speed jets of liquid are driven into the surface of a particle.[17] These jets and shock waves can cause surface coating removal as well as producing localized high temperatures and pressures.[26] Catalyst activity is therefore increased by catalyst surface deformation that exposes fresh, highly active surface and reduces the diffusion length in the catalyst pores. The local turbulent flow associated with acoustic streaming also improves mass transfer between the liquid phase and the surface, thus increasing the observed reaction rates.[12,27]

As an environmentally benign technique for the heterogeneous catalytic reduction, US is usually used to prepare catalytic materials and modify existing metal catalysts, as well as directly enhancing transformations.[28,29] Sonication has improved reaction rates in numerous reductions, but it is doubtful whether selectivity is improved by sonication.[28]

Microwave-assisted organic synthesis (MAOS) and the MW-assisted preparation of catalysts have also become very popular tools in the fields of green chemistry since 1986.[30-32] MW energy at the common frequency of 2.45 GHz (0.0016 eV) is too low to break chemical bonds and is also lower than the energy of Brownian motion.[33] Therefore, MW cannot induce, but can enhance chemical reactions.[34] MW-enhanced chemistry is based on the efficient heat transfer achieved by dielectric heating. This phenomenon is dependent on the ability of a specific material (solvent or reagent) to absorb MW energy and convert it into heat.[33] In contract to conductive heating, MW irradiation causes volumetric heating via the direct coupling of the electromagnetic field with molecules (solvents, reagents, catalysts) in the reaction mixture (minimized or no wall effect). As a result, fast selective heating can be attained by irradiating polar materials in a MW field.[33] MAOS can be also carried out under solvent-free conditions, enhancing reaction rates of cyclisation, aromatic substitution, oxidation, alkene synthesis, alkylation, decarboxylations, hydrogenation, radical reactions,

condensations and rearrangements.[35] As unique technique suitable for discovering and probing new chemical reactivity, MAOS is not only able to reduce chemical reaction times from hours to minutes, but it is also known to reduce side reactions, increase yields and improve reproducibility.[33] MW irradiation has proved itself to be a suitable energy source in catalyst preparation. Since the catalytic activity of the metal is strongly dependent on particle shape, size and size distribution,[36] like sonication, MW is also conducive to generating colloids and clusters on the nanoscale, and with greater uniformity.[37-39]

This review deals with the effects of US and MW on the catalyst preparation as well as reduction. As far as catalyst preparation is concerned, the advantages of sonication and MW irradiation, such as reductions in preparation time and excellent catalytic performance, are emphasized. The salient eco-friendly features of sonication and dielectric heating, namely the selectivity, experimental conditions and the reaction rates are discussed for selective catalytic reductions.

Zhilin Wu, after obtaining the PhD from The Friedrich Schiller University of Jena (FSU, Germany) in 2005, he continued working in The Institute of Technical Chemistry and Environmental Chemistry of FSU, and was engaged in the applications of ultrasound and microwaves in "Green Chemistry" and Environmental Remediation until Sept. 2012. Since 2013 he has been working as a researcher at the University of Turin (Italy). His work focused on understanding the mechanisms, kinetics, and energy efficiencies of degradation, oxidation, and hydrogenation of organic compounds driven by cavitation and microwaves.

Giancarlo Cravotto, after few years of experience in the pharmaceutical industry, he became a researcher in the University of Turin (Italy). He is currently Full Professor of Organic Chemistry and Department Director since 2007. His research activity is documented by more than 230 scientific peer-reviewed papers, several book chapters and patents. His main research interests are the synthesis of fine chemicals under non conventional techniques such as ultrasound, microwaves, flow chemistry and ball milling. He is the President of the European Society of Sonochemistry.

Emily Borretto undertook PhD studies in Medicinal Chemistry at the University of Turin (Italy)

working in the field of design and synthesis of new potential drugs, obtaining her PhD in 2012. Afterwards, her research activity was focused on non-conventional technologies such as ultrasound and microwaves for innovative green syntheses. Currently she has a post-doctoral position at the University of Turin.

Jonathan Medlock completed a PhD in organic synthesis with Stuart Warren at Cambridge University (UK). After a post-doctorial position in homogeneous catalysis with Andreas Pfaltz (University of Basel, Switzerland) he spent 7 years with the Catalysis and Chiral Technologies group of Johnson Matthey. He joined DSM in Basel, Switzerland in 2009 and is currently a Senior Scientist and Laboratory Head in the Process R&D group.

Werner Bonrath studied chemistry in Bonn and Münster (Germany) and moved to the MPI (Mülheim, Germany) to complete his PhD with Günther Wilke. He joined Hoffmann-La Roche in 1989 working in the area of catalysis for vitamins, carotenoids and fine chemicals. He completed his habilitation at the Univeristy of Jena (Germany) in 2007 and is currently a lecturer there and at the University of Basel. Since the merger with DSM, he is Competence Manager Heterogeneous Catalysis. In 2013 he received the Senior Industrial Investigator Award of the Swiss Chemical Society.

Part 1. Ultrasound applications

1.1 Ultrasound-assisted preparation of catalysts for reduction

Sonochemistry is the use of US to induce, enhance or alter chemical reactions. In addition to triggering free radical reactions, US has a mechanical impact on reactions, such as increasing Raynolds numbers, turbulent flow, and increasing the surface area between reactants, accelerating dissolution and/or renewing the surface of a solid reactant or catalyst.[40] Sonication for the preparation of catalysts has been shown to enhance the robustness, enantioselectivity and activity of the catalyst.[41-43]

Table 1. Summary on the US-assisted preparation of catalysts for reduction						
No.	Catalysts	Raw materials	US conditions	Characterization	Applications	Ref.
1	Ru-B amorphous alloy	RuCl$_3$, KBH$_4$, NaOH solution.	20 kHz, 60 W.	Non-porous structure particles <10 nm average size.	Reduction of maltose to maltitol.	[51]

#	Catalyst	Reagents	Sonication conditions	Observation	Application	Ref.
		$(NH_4)_2RuCl_6$, KBH_4.	20 kHz, 60 W.	Nanoparticles from 2.4 to 4.9 nm.	Liquid-phase maltose reduction.	[67]
2	Ru-B-X/SBA-15	$(NH_4)_2RuCl_6$, SBA-15 KBH_4.	20 kHz, 60 W.	Nanoparticles with high surface, homogeneously confined in the porechannel of SBA-15.	Liquid-phase maltose reduction.	[68]
3	Ni-B amorphous alloy			The catalyst surface becomes homogeneous, the coverage of Ni centers decreases, and the surface area slightly increases.	Selective reduction of acetophenone to 1-phenylethanol.	[63]
4	La-doped Ni-B	KBH_4, NaOH, aqueous $NiCl_2$, $La(NO_3)_3$.		Particle sizes decreases from < 100 nm to < 70 nm.	Liquid-phase selective reduction of benzophenone to benzhydrol.	[69]
5	Ni-La-B/γ-Al_2O_3 and Ni-La-B/SiO_2[70]	Calcined SiO_2 or γ-Al_2O_3, $NiCl_2\cdot6H_2O$, $La(NO)_3\cdot6H_2O$, KBH_4.		More active Ni centers and hydrogen desorption on Ni-La-B/γ-Al_2O_3 than on Ni-La-B/SiO_2.	Reduction of benzophenone.	[71]
6	Ultrafine Co-B amorphous alloy	$CoCl_2$, KBH_4, NaOH aqueous solution.	28 kHz, 20 min.	Particles size <10 nm uniform distribution, increase in the specific surface area.	Liquid phase selective reduction of cinnamaldehyde (CMA) to cinnamyl alcohol (CMO).	[72]
		25% $NH_3\cdot H_2O$ solution, $CoCl_2$, BH_4^- in aqueous solution[62]	50, 5 or 100 W, 30 or 90 min.	Uniform spherical particles, strong electronic interaction between Co and B, strong hydrogen adsorption on Co active sites.	Liquid phase selective reduction of cinnamaldehyde (CMA) to cinnamyl alcohol (CMO).	[[62]
7	Co-Fe/diatomite	Diatomite, $Fe(NO_3)_3$, $Co(NO_3)_3$, H_2.	5 h.	Finer amorphous Co and Fe dispersion on the diatomite carrier. BET surface area and the contact surface with the carrier further increase.	Selective reduction of CMA to CMO.	[73]
8	Cu-Cr oxide and Cu-Cr oxide / TiO_2	$K_2Cr_2O_7$, $CuAc_2$ and NH_3 with or without $(Me_2CHO)_4Ti$ in aqueous solution.	20 kHz, 3 h, 100 W/cm^2.	Smaller particles that increase the specific surface area.	Liquid phase reduction of furfural to furfuryl alcohol.	[74]
9	3% Pt/C	Activated charcoal in HNO_3 solution, chloroplatinic acid aqueous solution, 95% ethanol	40 kHz, 250 W, 10-120 min.	Increased mesopore volume and adsorption of Pt precursor.	Reduction of o-chloronitrobenzene.	[75]
10	Pt/SiO_2, Pt/Al_2O_3, Pt/C and EuroPt-1(6% Pt/Silica)	Pre-treatment by US before their uses for reduction.	20 kHz, 30 W.	Sonochemical pre-treatment produces smaller metal particles and more uniform size distribution.	Selective reduction of CMA to CMO.	[76]
11	Pd cross-linked chitosan	Pd(II)-species with $NaBH_4$, resulting in a supported Pd(0) catalyst on chitosan.			Selective MW-assisted hydrogenation of α,β-unsaturated carbonyl compounds and other functionalities (alkynes, imines).	[86-87]

Near an extended solid surface, the non-spherical cavity collapse drives high-speed jets of liquid into the surface, causing catalyst damage and an increase in the number of edges, crevices and kinks that expose fresh and highly active surfaces.[21] This process can produce newly exposed, highly heated surfaces. In contrast, shock waves can accelerate solid particles to high velocities during the sonication of liquid-powder slurries. The resultant inter-particle collisions are capable of inducing dramatic changes in surface morphology, composition and reactivity.[16] Therefore, US has been used as a successful tool for the synthesis of catalysts and catalytic materials in order to improve catalyst activity and enhance the dispersion or crystallization process. Sonication not only leads to substantial reductions in overall preparation time,[44-47] but also creates smaller particle sizes, higher metal dispersion and favours catalyst stability.[46,48] Catalyst preparation is usually a time consuming process. For example, the preparation of vanadium phosphorus mixed oxides (VPO) involves the reduction of V_2O_5 in a mixture of isobutanol and benzyl alcohol under reflux for 12–14 h, followed by refluxing in phosphoric acid solution for an additional 6–8 h.[45] The sonication of the mixture can significantly reduce the preparation time of Ce-promoted VPO catalysts to a total of around 6 h. Pillai et al. [47] also demonstrated that the active VPO catalyst could be prepared in a relatively short time (3-6 h) via sonication as compared to conventional methods (20 h). At the same time, there was no deterioration in the catalytic properties during the liquid phase hydrogen peroxide oxidation of cycloalkanes in acetonitrile. In another example, synthetic zeolites were hydrothermally prepared via the heating of an aqueous solution of sodium silicate and sodium aluminate, at a temperature range of 25–300 °C, for a few hours to several days. Sonication led to substantial reductions in nucleation time (1 h, probe system) and overall completion times (3 or 4 h, probe system) compared to control reactions (5 h nucleation time and 10 h to completion).[44]

Besides reducing preparation time, sonication mainly changes catalyst morphology and particle size[49] thanks to the unique cavitation bubble implosion effect.[21,50] Meanwhile, strong shock waves and micro-jets, that can move at over 400 km/h, that are created by cavitation bubble implosion can crush catalyst particles and suppress agglomeration, resulting in finer and more dispersed catalyst particles.[51] The sonochemical decomposition of volatile organometallic compounds produces high surface area solids that consist of nanometer cluster agglomerates,[52] such as nanosize MoC, MoS_2, or Fe[53-56] or noble metal catalysts.[57,58] Sonication was also found to be efficient in the preparation of supported Ru and Pd samples as well.[59,60] Particle size can generally be controlled by adjusting the sonication power or time.[61,62] Pei et al.[25] reported the US-assisted synthesis of metal-metalloid amorphous alloys in which the US-assisted reduction gave rise to mono-dispersed and spherical Ru–B nanoparticles with a much smaller size of 2.4–4.9 nm than the broadly distributed particles of 15–50 nm prepared conventionally. In addition, the US-assisted method can induce a higher surface elemental B/M ratio. The increased surface B content can invoke a stronger electronic interaction with metal (M) and higher thermal stability by impeding the migration of the metal atoms. Furthermore, Chen et al.[63] synthesized a Ni–B nano-array replicated from mesoporous siliceous SBA-15. The silica-free Ni–B nano-array is constructed of hexagonally packed nanowires

4

with a uniform diameter of about 5 nm, which exhibit superior catalytic properties to their nanoparticle counterparts in the selective reduction of acetophenone to 1-phenylethanol. The ultrasonically prepared Co/SiO$_2$ catalyst also showed smaller crystallite size (3.8 nm) and higher metal dispersion compared to the catalyst prepared by the classical incipient wetness impregnation method (crystallite size = 6.9 nm).[48] Sonication appreciably enhanced the catalyst activity thanks to nanostructures as well as the increasing number of active sites and surface area of catalyst particles.[64] The sonochemical reduction of nickel ions complexed with ethylenediamine or hydrazine leads to more active Ni–B catalysts than conventional Ni–B and Nickel-alloy catalysts.[65,66] The Ni–Mo–B prepared by ultrasonic reduction exhibited higher activity than the conventional amorphous alloy catalyst.[25] Moreover, the catalyst prepared by sonication exhibited excellent robustness. Co/SiO$_2$ prepared under US was deactivated by less than 10% in 4 days. In contrast, the catalyst prepared by a classical impregnation method is rapidly deactivated with a 40% loss in conversion in 4 days.[48] Common catalysts for selective catalytic reduction prepared using sonochemical protocols, are summarized in Table 1, and described as follows:

1.1.1 Ru-B amorphous alloy

The Ru-B amorphous alloy catalyst was prepared via the chemical reduction of RuCl$_3$ with KBH$_4$ in NaOH solution under 20 kHz and 60 W US.[51] This catalyst had a similar amorphous alloy structure, surface electronic state and active site nature as the Ru-B catalyst obtained via chemical reduction, however, higher activity in the reduction of maltose to maltitol was observed thanks to smaller particle size. Sonication can effectively inhibit agglomeration, resulting in the formation of particles with less than 10 nm average size, compared to the 30-40 nm average size found in conventional reduction.

However, higher US power (100 W) led to particle agglomeration, resulting in more than 15 nm average particle size. This indicates that excessively high US power induces such intense catalyst particle collisions that agglomeration occurs, due to local hot fusion in the collision sites, causing increased particle size.[77] Since catalyst particles show a non-porous structure, active specific surface area is mainly determined by the catalyst particle size. Therefore, active specific surface area initially increased and then decreased with increasing US power. In the reduction of maltose, the selectivity to maltitol over a prepared Ru-B amorphous alloy catalyst reached 100% and activity was nearly 38 times higher than that of Nickel-alloy. Moreover, activity and selectivity were preserved for at least 6 reaction cycles, while the activity of the catalysts prepared by classic chemical reduction significantly decreased after only 5 runs. The more stable structure of the catalyst arose from the improved interaction between Ru and B under US. Meanwhile, sonication made the catalyst surface smoother, thereby inhibiting passivation and preserving catalytic activity.[51]

The sonochemical method was also applied to the synthesis of mono-disperse Ru-B amorphous alloy catalysts via the reduction of (NH$_4$)$_2$RuCl$_6$ using KBH$_4$.[67] The coordination of halide ligands to Ru^{3+} resulted in the formation of an ultrafine Ru-B amorphous alloy with high dispersion which exhibited much higher catalytic activity. The Ru-B nanoparticles were identified to be amorphous alloys ranging in size from 2.4 to 4.9 nm. The synthesized Ru-B catalyst was extremely active compared to the regular Ru-B catalyst which was obtained via the reduction of RuCl$_3$ with KBH$_4$ for liquid-phase maltose reduction. The catalytic

activity is about 11 times as high as industrial Nickel-alloy, and it was reused for 6 runs without significant deactivation.[67]

In a recent study, the Ru-B-X/SBA-15 catalyst was synthesized via the US-assisted incipient wetness infiltration of (NH$_4$)$_2$RuCl$_6$ into mesoporous siliceous SBA-15 and subsequent reduction with KBH$_4$.[68] This catalyst was identified to be an amorphous alloy which was highly dispersed within the pore channels of SBA-15. The Ru-B-X/SBA-15 catalyst was more active than the Ru-B-C/SBA-15 obtained via the same process but using RuCl$_3$ as the metal source for the liquid-phase maltose reduction. The Ru-B amorphous alloy nanoparticles possessed higher surface B content and were homogeneously confined in the pore channel of SBA-15, resulting in a catalytic activity which was up to 7 times as high as the reference unsupported Ru-B-C catalyst prepared via RuCl$_3$ reduction with KBH$_4$. No significant deactivation was observed after 11 runs, due to the improved thermal stability and stronger interaction between Ru-B and SBA-15. However, a significant loss in activity (74%) was observed for Ru-B-C after only 5 recycles. Furthermore, no Ru leaching was detected for the Ru-B-X/SBA-15 and Ru-B-C catalysts over repetitive uses. The transformation from an amorphous alloy structure to a crystalline structure has proven to be the reason for the deactivation of Ru-B-C.

1.1.2 Ni-catalysts

The hexagonally packed Ni-B amorphous alloy nano-array was prepared using US-assisted reductive-infiltration. This catalyst exhibited superior performance in the selective reduction of acetophenone to 1-phenylethanol.[63] It was suggested that the agglomeration was inhibited by sonication wherein the surface of the catalyst becomes homogeneous and the coverage of Ni centers decreases correspondingly. Sonication also slightly increased surface area. Fortunately, sonication did not change the amorphous structure of the Ni–B catalyst.[69]

In a recent investigation, a La-doped Ni-B catalyst had smaller particle size and more active centers, thus the ultrasonically prepared Ni-La-B catalyst was found to have better catalytic performance than the Ni-B catalyst for the liquid-phase selective reduction of benzophenone to benzhydrol.[69] The conversion of benzophenone using a Ni–B catalyst was 35% and the selectivity for benzhydrol was 92%. For comparison, the conversion of benzophenone over the Ni–La–B catalyst sharply increased to 84% while selectivity decreased slightly to 90%. Conversion increased to 100% and the selectivity was 90% using the Ni–La–B catalyst prepared by sonication. By contrast, conversion with Nickel-alloy catalyst was only 31% and the selectivity was 78%. It was proposed that the sonication prepared Ni–La–B catalyst particles were more dispersed and particle sizes decreased from < 100 nm to < 70 nm with higher catalyst surface area and H$_2$ –chemisorption.[69]

Ni–La–B nanoparticles showed high activity and selectivity thanks to the synergistic effect between La addition and sonication, but exhibited poor stability for recycling. Therefore, SiO$_2$ with its planar structure and γ-Al$_2$O$_3$ with its porous structure were used as supports to improve the conversion of benzophenone and catalyst stability.[71] Benzophenone conversion increased by about 15% when using the US prepared catalyst. The sonication made the particle size smaller and enhanced the dispersion of active particles over the carriers, preserving the amorphous structure of Ni–La–B catalysts.[78,79]

It was suggested that sonication inhibited the agglomeration of Ni–La–B particles on both carriers, and Ni–La–B amorphous alloy particles were homogeneously dispersed on the surfaces of

SiO$_2$ and γ-Al$_2$O$_3$. Moreover, sonication improved the surface Ni^0 content on SiO$_2$ leading to more active centers. In contrast, sonication lowered Ni^0 and Ni^{2+} content on the porous structured γ-Al$_2$O$_3$ and improved the dispersion of active component, as well as the migration of small Ni particles into the pores of γ-Al$_2$O$_3$. The porous structure of γ-Al$_2$O$_3$ also resulted in more active Ni centers and more hydrogen desorption on Ni-La-B/γ-Al$_2$O$_3$ than on Ni-La-B/SiO$_2$.[70] The Ni-La-B amorphous alloy on SiO$_2$ prepared under US, showed higher initial activity and selectivity than those on γ-Al$_2$O$_3$; whereas Ni-La-B on SiO$_2$ showed poor stability compared to Ni-La-B/γ-Al$_2$O$_3$. It was proposed that the adsorption of reactants and products onto the catalyst surface leads to the coverage of the active Ni sites and deactivation of Ni-La-B on SiO$_2$. Ni-La-B on γ-Al$_2$O$_3$ prepared under US exhibited lower, but stable activity with a slight selectivity decrease.

As a pre-electrolytic treatment, US was also applied to the electrocatalytic hydrogenation of benzaldehyde in water.[80] With a nickel matrix, the effect of US led to an increase of 5% in the hydrogenation yields. It was proposed that a Ni matrix together with US pre-electrolysis treatment allowed a nano-structured nickel deposit to form on the cathode surface. Smaller particles have more edges and kinks, which improve the surface reactivity.

1.1.3 Co-catalysts

An ultrafine Co-B amorphous alloy was prepared via CoCl$_2$ reduction with KBH$_4$ in a NaOH aqueous solution, then sonicated at 28 kHz and finally processed at various temperatures.[72] Co-B amorphous alloy showed spherical particles of about 20 nm average particles size without sonication, but the size distribution was not uniform. Due to the ultrasonic dispersion, Co-B amorphous alloy formed finer particles with an average particle size of less than 10 nm and the distribution was very uniform after 20 min sonication. This resulted in a significant increase in the specific surface area and catalytic activity. However, longer sonication time (e.g. 25 min) led to the occurrence of significant catalyst particle agglomeration, resulting in larger Co-B particle size, smaller specific surface area and lower catalytic activity. This was caused by local high temperatures and extreme collision conditions generated by the collapsing cavitation and micro-jets.

The ultrafine Co-B amorphous alloy prepared under US was applied in the liquid phase selective reduction of cinnamaldehyde (CMA) to cinnamyl alcohol (CMO) and showed full selectivity to CMO (100%), see Scheme 1. The sonication not only maintained the structure of Co-B amorphous alloy, but also showed high selectivity for the hydrogenation of C=O rather than C=C bonds. Catalytic activity and CMO yield significantly increased with increasing sonication time for catalyst preparation. Reaction activity (including the initial hydrogen absorption rate and CMA's conversion rate in 90 min) gradually increased and the CMO yield reached its highest value (70%) with the catalyst prepared by 20 min sonication. In contrast, using the catalyst prepared under silent conditions, CMO yield decreased to 42%.The CMO yield was 64% using the catalyst prepared by 25 min sonication.

Sonication was also directly applied during the reduction of Co(NH$_3$)$_6$$^{2+}$ with BH$_4$$^-$ in aqueous solution to prepare uniform spherical Co-B amorphous alloy nanoparticles.[62] The intense shock waves and extremely high energy level of localized supersaturation induced by cavitation collapse inhibited the agglomeration of particles and triggered nucleation, resulting in the formation of uniform spherical Co-B particles.[77,81] However, the Co-B particle size increased with increasing US power and sonication time due to the melting agglomeration.[24] Thus, optimal

sonication conditions ensured the preparation of a catalyst with superior performance, which had a significantly greater metallic area and better Co-B particle dispersion and Co active sites. It was proved that the US-prepared Co-B catalyst exhibited much higher activity than the regular Co-B obtained via the direct reduction of Co^{2+} with BH$_4$$^-$ for liquid-phase CMA reduction. Meanwhile, the higher selectivity for CMO was obtained due to the uniform spherical particles of Co-B amorphous alloy and the strong electronic interaction between Co and B, which enhances the competitive adsorption of C=O group against C=C group in the CMA molecule. Moreover, the stronger hydrogen adsorption on Co active sites was more favorable for C=O hydrogenation rather than C=C hydrogenation.

In addition, a Co-Fe/diatomite catalyst was ultrasonically prepared for the selective reduction of CMA to CMO.[73] Diatomite was immersed in Fe(NO$_3$)$_3$ solution and sonicated for 5 h. Dried Fe^{3+}/diatomite was then immersed in a Co(NO$_3$)$_3$ solution and sonicated for 5 h. The dried Co^{3+}-Fe^{3+}/diatomite was calcinated for 3 h in the air atmosphere, and then reduced for 3 h in a hydrogen atmosphere to form the activated catalyst.

Sonication generated finer particles and Co and Fe particle dispersion on the diatomite carrier, which exhibited an amorphous trend. Meanwhile, BET surface area and the contact surface with the carrier further increased. Positron life is proportional to the electron density at positron annihilation. The active electronics are enriched at the locations with active centers on the catalyst surface, so that positrons are easily annihilated and positron life was shortened.[82] The positron lifetime on the sonication prepared Co-Fe/diatomite catalyst decreased, indicating active electron enrichment on the catalyst surface increased. The increasing number of defects on the catalyst surface reveals that effective catalyst dispersion was realized by sonication and more active sites on the catalyst surface were stimulated, increasing catalytic activity.[73]

As a result, Co-Fe/diatomite sonication prepared catalyst enhanced the conversion of CMA and improved the selectivity of CMO. The conversion of CMA with US-prepared catalyst was 75% with 88% selectivity to CMO. In contrast, the conversion of CMA with conventionally prepared catalyst was 68% with 76% selectivity to CMO. The catalytic activity for reduction of CMA is consistent with the analysis of positron lifetime.

1.1.4 Copper-chromite oxide and TiO$_2$-supported copper-chromite oxide

Copper-chromite oxide and TiO$_2$-supported copper-chromite oxide catalysts were prepared by sonication for the liquid phase reduction of furfural to furfuryl alcohol.[74] The aqueous solutions containing K$_2$Cr$_2$O$_7$, CuAc$_2$ and NH$_3$ with or without (Me$_2$CHO)$_4$Ti were sonicated for 3 h at 20 kHz frequency and 100 W/cm^2 power intensity. The product was washed, dried and then calcinated. The catalyst particles prepared by sonication are smaller than those under silent conditions, increasing the specific surface area. Due to the effect of US, the CuCrO$_4$ formed is highly dispersed on amorphous titania and the agglomeration of CuO and CuCr$_2$O$_4$ particles were inhibited with TiO$_2$, resulting in the formation of finer CuO and CuCr$_2$O$_4$ particles.

Despite the content of Cu and Cr decreasing, TiO$_2$-supported catalysts showed higher activity than the TiO$_2$-free catalyst, which had no activity at 140 °C after US activation and only poor activity at 170 and 200 °C. By contrast, these TiO$_2$-supported catalysts by calcination and US activation exhibited a catalytic activity at 140 °C, and the catalyst prepared by sonication shown higher activity.[74]

1.1.5 Pt-catalysts

Pt/C catalysts with 3% metal loading were prepared under US and applied for *o*-chloronitrobenzene reduction.[75] Compared with the activated charcoal treated by conventional method, US led to a decrease in specific surface area, total pore volume and ash content, while an increase in pH value, the mesopore volume and specific mesopore surface area were observed, so as to increase the surface area available for adsorption of the metal precursor, thereby increasing the dispersion of Pt particles and reducing the particle size of metal particles.

The microstructure of activated charcoal consists of macropores (> 100 nm), mesopores (2 nm-100 nm) and micropores (< 2 nm). The specific surface area is mainly constituted of micropores. When the adsorbate diameter is more than 1/3 pore diameter, adsorbate movement is blocked, decreasing the adsorption capacity. Metal precursor adsorption onto activated charcoal is mainly affected by mesopores rather than micropores. US makes fewer micropores and more mesopores, increasing the mesopore volume and the adsorption of Pt precursor. Therefore, metal dispersion is enhanced, reducing the particle size of metal particles. Furthermore, sonication enhanced the reaction of nitric acid with activated charcoal, inducing a large number of oxygen-containing functional groups on the activated charcoal surface that can be used for adsorption. This resulted in a higher activated carbon cation exchange capacity, which is favourable for high Pt metal particle dispersion on the support and an increase in catalyst activity.

The cavitation bubbles not only destroy the adsorption of attachments onto the activated charcoal surface, but also cause damage to the unstable oxygen-containing adhesion layer. The cavitational effects result in adhesion matrix desorption from the surface and its dispersion into the solution, causing a decrease in ash content on the surface of activated charcoal. The destruction of unstable acidic oxygen-containing groups reduces the acidity of the carbon surface and pH increases. The cavitation bubbles destruct micropores and create mesopores, resulting in a decrease in specific surface area and total pore volume. Long sonication converts mesopores to macropores, so pore volume and the specific surface area of mesopores initially increase and then decrease. Pt/C catalyst activity is directly related to the mesopore volume, pH value and ash content rather than the specific surface area and total pore volume. Under alkaline conditions and in a xylene solvent, the liquid-phase hydrogenation of *o*-chloronitrobenzene was carried out for the preparation of 2,2-dichloro hydrazobenzene Both hydrogen absorption and conversion rate with conventionally prepared catalyst were low, while the US-prepared catalysts obviously enhanced the hydrogen absorption and conversion. The optimal sonication time for catalyst preparation is 60 min with maximum hydrogen absorption capacity and conversion rate.[75]

The catalysts such as Pt/SiO$_2$, Pt/Al$_2$O$_3$, Pt/C and EuroPt-1(6% Pt/Silica) were pre-treated using sonication before their uses for reduction.[76]

Sonochemical pre-treatment was highly beneficial for the selective formation of CMO (up to 80%) over Pt/SiO$_2$ catalysts, besides the significant increase in reduction rate (two-fold) under mild experimental conditions (60 °C, 1 bar). The reaction rates decreased over Pt/C and Pt/Al$_2$O$_3$. Pt/Silica (EuroPt-1), which is a well-known reference catalyst, gave similar changes after sonication to 3% Pt/SiO$_2$, proving the crucial role of the SiO$_2$ support. Moreover, the prolonged sonication does not cause further rate increases; the rate increased to 0.07 mol/g$_{Pt}$/h (in

contrast with 0.03 mol/g$_{Pt}$/h obtained in the "silent" reaction), but remained steady after longer irradiation. In parallel, the selectivity for CMO formation also remarkably increased. The non-treated catalyst produced only 40% CMO, while pre-sonication resulted in a two-fold increase (80% overall selectivity) in CMO formation.

Due to the mechanistic effects of sonication, sonochemical pre-treatment produces smaller metal particles and more uniform size distribution, as is in agreement with earlier findings.[44,83] The decrease in metal particle size brought about by ultrasonic pre-treatment resulted in lower selectivity in the formation of CMO in the presence of Pt/C and Pt/Al$_2$O$_3$ catalysts. However, ultrasonic pre-treatment resulted in a remarkable difference in the chemoselectivity with Pt/SiO$_2$. Namely, C=O hydrogenation became the major reaction path, producing CMO in higher yield and selectivity. As a result of the significant support effect, the beneficial role of ultrasonic pre-treatment in enhancing activity and selectivity was interpreted by assuming the formation of effective metal-support active centres over silica, which provide stronger acceptor sites for C=O adsorption.[84,85]

1.1.6 Pd cross-linked chitosan

Chitosan has been efficiently cross-linked with hexamethylene diisocyanate (HMDI) in the presence of suitable metallic salts in solution under intense sonication. The new metal loaded solid chitosan derivative was then successfully applied as a catalyst support for the Suzuki reaction as well as for copper-catalyzed cycloaddition reactions between azides and alkynes.[86] The polymer was then subjected to chemical reduction of the immobilized Pd(II)-species with NaBH$_4$, resulting in a supported Pd(0) catalyst. The catalyst was characterized by FT-IR and elemental analysis of the metal content was determined by ICP-MS measurements.

This US-prepared catalyst was efficiently applied in the selective MW-assisted hydrogenation of α,β-unsaturated carbonyl compounds and other functional groups (alkynes, imines).[87] This process incorporated both MW and US techniques. These types of catalysts proved to be highly active.

1.2 Ultrasound-assisted selective reductions

US-assisted organic synthesis is a "green" technique which is applied in many organic synthetic routes giving great advantages in terms of high efficiency, low waste generation (clean reaction) and energy saving (short reaction time). [84,88] Sonochemistry promotes chemical reactions and enhances mass transfer. It offers the potential for shorter reaction cycles, cheaper reagents, and milder reaction conditions.[13,16,89-92] The advantages of US in chemical reactions could be applied in industrial application in pharmaceutical or fine chemical industry. Sonochemistry can be used for fast reactions or in the synthesis of expensive products.[93,94] Therefore, sonication is a promising technique for driving reactions, including heterogeneous selective hydrogenation, at a high rate and with good selectivity.[11,20,95] Nowadays, US is not only applied to prepare catalysts, but also directly to enhance and improve the conversion and selectivity of reduction.[76,96]

The chemical effects of US are diverse and include dramatic improvements in both stoichiometric and catalytic reactions. For heterogeneous systems proceeding via ionic intermediates, the reaction is influenced primarily through the mechanical effects of cavitation such as surface cleaning, particle size reduction and improved mass transfer.[40,97,98] Here the role of US should be more or less similar to that of high-speed stirrers.[16] The

mechanical effect originates from the asymmetric collapse of cavitation bubbles near the liquid-solid phase boundary disrupting the interface and impelling jets of liquid into the catalyst surface (liquid jet impingement),[21,99] leading to the grinding of solid catalysts to become smaller particles, revealing new, previously unexposed surface and therefore, resulting in a dramatic increase in surface area, dispersion and BET surface area.[100] Increased adsorption/desorption rates of either liquid species at the catalyst surface or gas dissolution in the liquid phase may also enhance/alter reaction outcome. Furthermore, solid catalyst inter-particle collisions may yield highly active sites and unique US-assisted chemical modifications.[99] Thus, volatile reactants are brought into contact with clean surfaces, and solids, which may be unreactive due to high lattice energy, are induced to participate in chemical reactions.[16] Therefore, acoustic cavitation and microstreaming at the surface are both significant in heterogeneous solid-liquid systems. The former produces high speed microjets of liquid which impinge upon the surface and cause surface erosion and localized heating. The latter creates turbulent flow and can significantly improve mass transport between solution and surface.[16] Finally, collapsing cavitation bubbles act as a localized microreactor with high temperatures and pressures, which behave as extreme autoclave conditions.[22,64]

The salient advantages of the US method include reductions in catalyst loading and reaction time, when compared to the conventional methods involving heating and stirring.[15,43] In addition, a large number of significantly positive effects that sonication can have on activity were demonstrated in heterogeneous catalytic reductions:[76,101,102] such as the hydrogenation of diphenylacetylene over palladium hydrazine in a common US cleaning bath at 25 °C;[10] 1-phenyl-1,2-propanedione over cinchona alkaloid modified 5 wt.% Pt/silica fiber catalyst in mesitylene at 158 °C under hydrogen pressure of 10 bar;[41] citral to citronellal over a Nickel-alloy catalyst in isopropanol at the operating pressure 50 bar and at 70.8 °C[17,98] ethyl pyruvate over 3 wt.% Pt/SiO$_2$ catalyst in ethanol at 25.8 °C;[101] soybean oil under 8.5 bar hydrogen pressure;[103] cinamaldehyde over Pt/SiO$_2$ catalyst at 1 bar;[104] oct-1-ene over 10% Pd/C catalyst at 25.8 °C in absolute ethanol[105] a carbonyl group of ethyl 9-(2,3,4-trimethoxy-6-methylbenzoyl)nonanoate with ultrasonic flux density 1 W cm^2 for 30 s[106] olefins using formic acid as the hydrogen transfer agent over 10% Pd/C at 25.8 °C with a toluene solvent in an ultrasonic cleaning bath[107] as well as the reduction of aromatic nitro compounds to the corresponding amines and reductive coupling of aromatic ketones over samarium/ammonium chloride[108,109] or aluminum/ammonium chloride.[110]

Kulkarni and Török recently reviewed the application of US activation in heterogeneous catalytic hydrogenations.[28] In many cases, sonochemical activation also resulted in selectivity enhancement; such as in the hydrogenation of α-ketoesters on cinchona alkaloid modified Pt/Al$_2$O$_3$ catalyst,[115] 3-buten-1-ol

Table 2. Summary on the US-assisted selective reductions

No.	Reactions	Catalysts and reactants	US conditions	Advantages	Ref.
1	Hydrogenation of olefins	5%Pd/C catalyst, olefin, anhydrous hydrazine, and absolute ethanol (additional benzene) under N$_2$ atmospheric pressure.	US bath (150 W, 55 kHz).	For diphenylacetylene hydrogenation, a 75% yield by sonication in an US bath in 1 h, while a 24% yield with stirring in 1 h.	[10]
2	CMA to CMO	Supported platinum catalysts, 2-propanol, cinnamaldehyde.	Realsonic 40SF US bath (20 kHz, 30 W); Sonics&Materials VC 50 US processor with a 3 mm wide and 138 mm long titanium alloy probe.	Sonication resulted in a two-fold increase (~80% overall selectivity compared with 40 %) in CMO formation.	[91]
		Pd-black and Nickel-alloy catalysts, cinnamaldehyde, isopropanol with 8.5 atm of H$_2$ pressure.	1.3 cm diameter US probe (20 kHz, 340 W).	The sonicated activities compared to the blank were 9-fold and 20-fold greater for the Pd-black and Nickel-alloy catalysts, respectively.	[99]
		Ru-B amorphous alloy, cinnamaldehyde and ethanol under atmospheric H$_2$ pressure.	US bath (28 or 48 kHz, 30 W/cm^2) at 70 °C.	Sonication greatly enhanced the reaction rate and maintained the excellent selectivity to CMO.	[100]
3	Asymmetric hydrogenation of isophorone	5% Pd/ Al$_2$O$_3$, (S)-proline, MeOH, and substrate.		The presonication of a commercial Pd/ Al$_2$O$_3$-proline catalytic system under 10-80 bar hydrogen pressure at 25 °C resulted in highly enhanced enantioselectivities (up to 85% ee).	[111]
4	3-buten-2-ol to 2-butanol	Pd-black was reduced with hydrogen (80 psig) in water using US for 4 min prior to reaction.	20 kHz at an average power of 360 W (electrical; 90% amplitude).	Selectivity showed a 7-fold increase toward 2-butanol formation and activity was enhanced by a factor of 10.8 compared to the non-cavitating high-power US experiment.	[112]
5	Citral to citronellal and citronellol	Nickel-alloy in 2-propanol, in an automatic laboratory-scale reactor, operating at 50 bar and at 70 °C.	20 kHz, 0-100 W, 8–20 W /100 ml, or related to the tip area of the probe (1.54 cm^2) 13– 32 W/cm^2.	Sonication increased reaction rate and enhanced selectivity. The optimum reaction time is shorter (around 80 min) than when no acoustic irradiation (close to 200 min).	[98]
6	Hydrogenation of soybean oil	Copper chromite or nickel catalysts.		Hundredfold Increased in a US continuous system. With US, 87% hydrogenation of linolenate in soybean oil was obtained in 9 sec at 8 bar H$_2$ with 1% copper chromite at 181 °C and 77% linolenate hydrogenation with 0.025% nickel.	[103]
		0.02% nickel catalyst or 50 ppm nickel in the oil under 1 to 6 bar H$_2$.		After 20 min, the average reaction rate was about five times faster with sonication.	[113]
7	Reduction of aryl nitro compounds	Iron powder in a solvent mixture of ethanol, acetic acid and water in an air atmosphere at 30 °C.	US bath (35 kHz, 85 W).	Sonication drastically accelerated the iron-catalyzed reduction of the aryl nitro functionality in the presence of these reduction sensitive groups.	[114]

aqueous solutions over Pd black,[116,117] CMA over Pd black and Nickel-alloy,[99] Z-2-buten-1-ol and Z-2-penten-1-ol on Pd-black,[118] and D-fructose to D-mannitol over Cu/ SiO$_2$.[119]

Several examples of selective catalytic reductions that can be improved using US are summarized in Table 2 and reviewed as follows:

1.2.1 Alkyne hydrogenation

Selectivity control between semi-reduction and over-reduction is a difficult issue in the partial hydrogenation of alkynes. Lindlar and Dubuis demonstrated the unique role that the palladium catalyst with lead-doping plays in the partial hydrogenation of alkynes.[120] High selectivity has been achieved by controlling the amount of H_2 consumed.[121] Nowadays, as the need for health and environmental protection increases, the design of alternative and/or lead-free catalysts for the existing semi-hydrogenation systems has received increasing attention as a means to achieve similar reproducibility, higher chemoselectivity and catalyst recyclability.[28] Such catalysts include phosphinated polymer incarcerated (PI) palladium catalysts,[122] nickel(0) nanoparticles,[123] zinc and ammonium chloride,[124] non-precious metal alloys,[125] ruthenium (II) phosphine/mesoporous silica catalysts,[126] and Au/Al_2O_3 and Au-Ni/Al_2O_3 nanocomposites, and BASF's NanoSelect Pd catalysts.[127,128]

In 1985, the US-accelerated hydrogenation of olefins using a Pd catalyst and hydrazine under N_2 atmospheric pressure was reported.[10] In the hydrogenation of diphenylacetylene, a 75% yield was obtained by sonication in an US bath in 1 h, while a 24% yield was obtained with stirring in 1 h. The improvement may arise from increased catalyst surface area caused by the ultrasonic fragmentation of the carbon support, or from the sonic activation of the Pd surface. Moreover, strong agitation of the mixture resulting from the cavitation phenomenon produced large quantities of gas (presumably H_2 and N_2 from the decomposition of hydrazine). It indicated that the Pd-hydrazine couple is a very efficient hydrogen donor in the presence of US, and the rate of hydrogenation is significantly enhanced.

1.2.2 Cinnamaldehyde to cinnamyl alcohol

The US-assisted selective hydrogenation of CMA to CMO has been widely investigated. The possible hydrogenation pathways of CMA are illustrated in Scheme 1.

The reduction of CMA over a Ru-B amorphous alloy under sonication was performed in an US bath (28 or 48 kHz, 30 W/cm^2) at 70 °C and under atmospheric H_2 pressure.[100] Sonication inhibited the aggregation of Ru-B particles, leading to the formation of particle sizes of less than 40 nm and a narrow Ru-B particle size distribution. In a comparison, the pristine sample exhibited a scattered Ru-B particle size distribution ranging from 32 to 80 nm.

As a result, the BET of the Ru-B amorphous alloy catalyst was measured to be 15 m^2/g after hydrogenation without sonication and 20 m^2/g after hydrogenation with sonication for 6 h. The improved Ru-B catalyst dispersion enhanced the number of active sites exposed to the reactant. After hydrogenation, the chemical compositions and amorphous structure of the Ru-B catalyst did not change with or without sonication. Furthermore, no leaching of Ru from catalysts was observed after hydrogenation with sonication. Therefore, sonication not only greatly enhanced the reaction rate, but also maintained the excellent selectivity to CMO over the ultrafine Ru-B amorphous alloy catalyst. It needed 3 h to reach the maximum yield with sonication, whereas more than 6 h were needed to obtain the comparative yield in the absence of US. Moreover, the CMA hydrogenation rate slightly increased with increasing ultrasonic frequency from 28 to 48 kHz. Increasing sonication time significantly enhanced the hydrogenation, but did not change the selectivity to CMO.
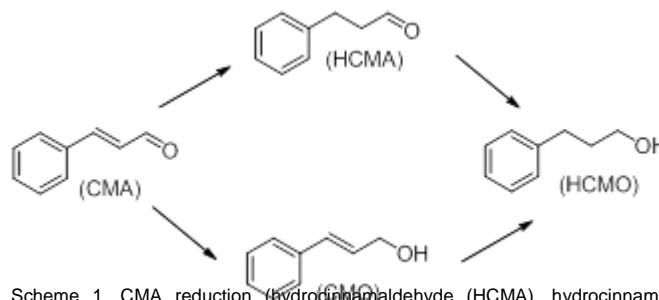
Scheme 1. CMA reduction (hydrocinnamaldehyde (HCMA), hydrocinnamyl alcohol (HCMO).[62]

The hydrogenation of CMA was also performed over Pd-black and Nickel-alloy catalysts at 25 ± 3 °C with a 1.3 cm diameter ultrasonic probe (20 kHz, 340 W).[99] Higher intermediate hydrocinnamaldehyde (HCMA) maximum relative concentration was formed in the US experiments compared to the stirred experiment. The activities of the sonicated experiments compared to the blank were 9-fold and 20-fold greater for the Pd-black and Nickel-alloy catalysts, respectively.

In another example, the chemoselective C=O hydrogenation of CMA was performed over supported platinum catalysts with sonication.[104] The sonication of the catalyst before the reaction resulted in changes both in reaction rates and product selectivity. Sonication resulted in a two-fold increase (~80% overall selectivity compared with 40 %) in CMO formation. Meanwhile, Török et al.[104] reported that the sonochemical pre-treatment in US bath (power not below than 30 W) increased the enantiomeric excess (e.e.) respect the non-treated catalyst for enantioselective hydrogenation of ethyl pyruvate. The best selectivity was obtained at 10 bar H_2 pressure after 30 min of pre-sonication (97.1±1% e.e.) while this was not observed at 1 bar. In contrast, a slight increase in e.e. % was observed when using the probe at under 10 bar, while no effect was observed working at under 1 bar. Therefore, the US bath was proved to be better for enantioselective hydrogenations than probe reactors.

The rate increase, independent of the reaction type, was interpreted on the basis of higher metal surface brought about by decreased particle size. The size of platinum particles on both supports decreased monotonically as a function of sonication time. The particle size distribution of the platinum crystallites in the pristine samples was of Gaussian type, while the distribution is close to homogeneous after sonication; the smaller metal crystallites became predominant. The potential of the promoted metal–support interaction contributed to increase the selectivity.

1.2.3 Asymmetric hydrogenation of isophorone

The sonochemical asymmetric hydrogenation of isophorone (3,3,5-trimethyl-2-cyclohexenone) by proline-modified Pd/Al_2O_3 catalysts has been reported.[111] The presonication of a commercial Pd/ Al_2O_3-proline catalytic system under 10-80 bar hydrogen pressure at 25 °C resulted in highly enhanced enantioselectivities (up to 85% ee, as shown in Scheme 2.

The presonication decreased the mean metal particle size from 4.1 nm to 3.2 nm (after 10 min), 1.8 nm (after 20 min), respectively. The surface cleaning effect of US enhanced both adsorption of the modifier and the modifier induced surface restructuring of the metal. Therefore, the major effect is enhanced adsorption of the chiral modifier as sonication removes surface impurities. The presonication results in enantioselectivity improvement only when both catalyst and modifier are present in

the solvent. "Modifier-free" presonication and presence of substrate during pretreatment decreased enantioselectivity. The optimum occurs when the catalyst/modifier system is sonicated in the solvent for 20 min. The presonication increased optical yields throughout the hydrogen pressure range.
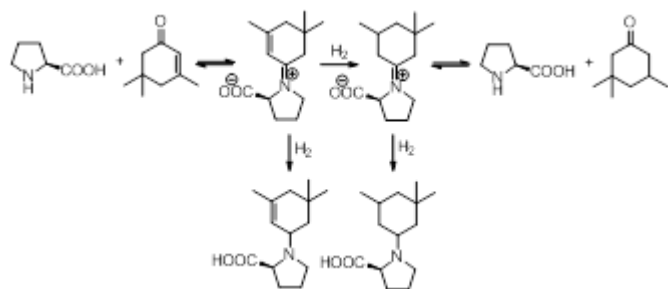
Scheme 2. Asymmetric hydrogenation of isophorone[111]

1.2.4 3-Buten-2-ol to 2-butanol

3-Buten-2-ol undergoes H-atom elimination and addition reactions on Pd-black to yield 2-butanone and 2-butanol, respectively. The hydrogenation profile of 3-buten-2-ol is illustrated in Scheme 3. The heterogeneous aqueous hydrogenation of 3-buten-2-ol over Pd-black catalyst was carried out at 22 °C under US (20 kHz) with the aim of enhancing 2-butanol production.[112] Meanwhile, 1-pentanol, used as an inert dopant, was added to promote cavitation effects during sonication (cavitating US) where it otherwise would not occur. Selectivity showed a 7-fold increase toward 2-butanol formation and activity was enhanced by a factor of 10.8 compared to the non-cavitating high-power US experiment.
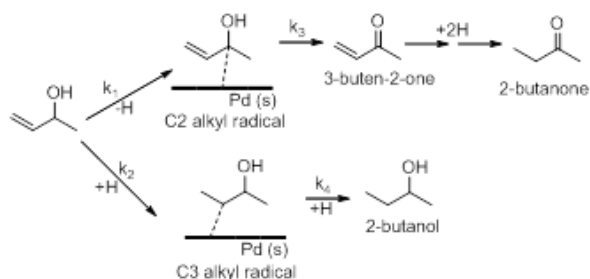
Scheme 3. Hydrogenation of 3-buten-2-ol[112]

The overall rates for cavitating US to non-cavitating US to stirred (without dopant) are about 53:5:1. This demonstrates that cavitation significantly enhances activity mass transport. In addition, the 5-fold enhancement in reaction rate for non-cavitating US compared to conventional agitation is significantly greater than the 37% increase in surface area.

1.2.5 Citral to citronellal and citronellol

Citral hydrogenation over a Nickel-alloy catalyst was carried out in isopropanol under US (20 kHz, 0-100 W) at 70 °C, with 50 bar hydrogen pressure.[98] The reaction scheme is depicted in Scheme 4.

Acoustic irradiation notably delayed catalyst deactivation in the hydrogenation of citral to citronellal and citronellol. Sonication thus increased reaction rate and enhanced selectivity. The combined yield of citronellol and citronellal is very close to unity,

slightly better with acoustic irradiation than with conventional hydrogenation. Moreover, the optimum reaction time is shorter (around 80 min) than when no acoustic irradiation is used (close to 200 min).
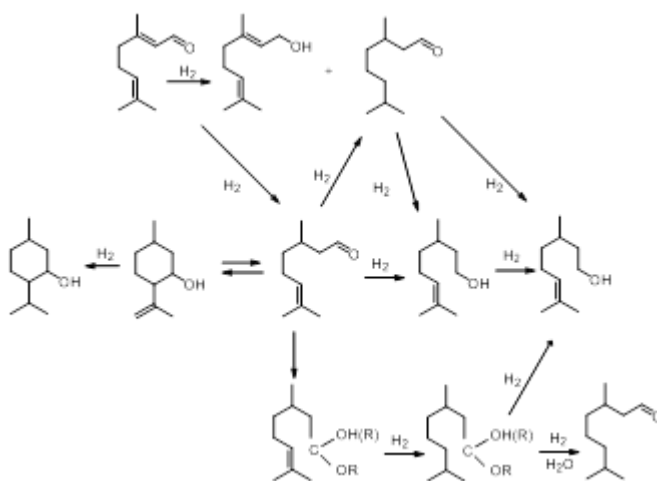

Scheme 4. Hydrogenation of citral[98]

1.2.6 Ultrasonic hydrogenation of vegetable oils

Industrial sonochemical reactors were pioneered more than 50 years ago by Saracco and Arzano,[129] who studied the US-assisted hydrogenation of unsaturated esters and described geometry and features of an optimized reactor. They demonstrated the huge influence of the reactor geometry on the kinetics of Raney-Ni catalyzed hydrogenation of olive oil.

The hydrogenation rate of soybean oil with either copper chromite or nickel catalysts increased more than a hundredfold under the aid of sonication in a continuous reaction system,[103] see Scheme 5.
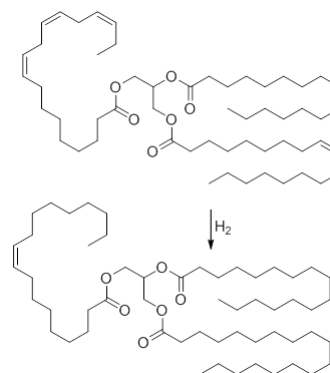

Scheme 5. Hydrogenation of soybean oil[130]

In a continuous reaction system, the selectivity for linolenate reduction with a copper catalyst was somewhat lower with sonication than under silent conditions. With US, 87% hydrogenation of linolenate in soybean oil was obtained in 9 sec at 8 bar H_2 with 1% copper chromite at 181 °C and 77% linolenate hydrogenation with 0.025% nickel. Without sonication, only 59% linolenate hydrogenation was obtained in 240 sec with copper chromite at 198 °C and 34 bar H_2 and 68% linolenate hydrogenation in 480 sec with nickel at 200 °C and 8 bar H_2.

Refined and bleached soybean oil was hydrogenated with and without sonication in a batch system.[113] Reactions were carried out at 170 °C with 0.02% nickel catalyst or 50 ppm nickel in the oil. Hydrogen pressure was varied from 1 to 6 bar. After 20 min, the average reaction rate was about five times faster with sonication. The hydrogenation rate generally increased with increasing hydrogen pressure using sonication. However, the increasing rate is more sinusoidal in nature than linear.

1.2.7 Selective reduction of aryl nitro compounds

The selective reduction of aryl nitro compounds in the presence of sensitive functionalities, including halide, carbonyl, nitrile and ester substituents, has been reported under sonication at 35 kHz giving yields of 39-98%.[114] The sonication was performed in a US cleaning bath (35 kHz, 85 W) in an air atmosphere at 30 °C. The reduction of aryl nitro compounds is known to proceed via the hydroxylamine, followed by azoxy and azo compounds, to its corresponding aryl amine after a prolonged reaction time (Scheme 6).[131]
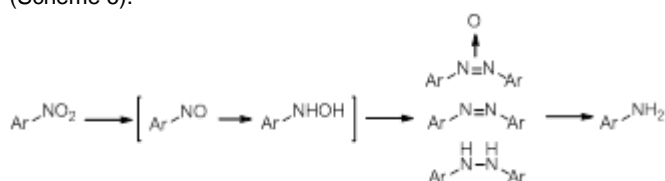
Scheme 6 Reduction of aryl nitro compounds[114]

Iron powder proved superior to stannous chloride as it gave high tolerance to sensitive functional groups and high yields of the desired aryl amines in relatively short reaction times.

Sonication drastically accelerated the iron-catalyzed reduction of the aryl nitro functionality in the presence of these reduction sensitive groups. In addition, the reaction of aryl nitro compounds with iron powder in a solvent mixture of ethanol, acetic acid and water promoted by sonication provides a much more accessible and simpler procedure.

The high energy effects of acoustic cavitation in addition to the continuous cleaning of the iron surface are responsible for the enhanced reaction rate. The later probably accounts for the greatest enhancement in reaction rate since surface impurities such as oxides, hydroxides and carbonates inhibit contact between the aryl nitro and the iron surface under thermal heating.[20] In addition, the cleaning of iron sweeps reactive intermediates or products from the surface making way for subsequent reactions.[132]

Part 2 Microwave applications

Several examples of MW applications (both in catalysts preparation and in selective catalytic reductions) are summarized in Table 3 and reviewed as follows.

2.1 Microwave-assisted preparation of catalysts for selective reductions

In recent years, the MW-assisted preparation of metal nanoparticles has been investigated with the aim of achieving greener protocols characterized by shorter reaction times, reduced energy consumption and higher yields.

Table 3. Summary of MW catalysts preparations and applications.

No.	Catalyst	Raw materials	Preparation MW conditions	Characterization Av. Diam. (nm)	BET (m²/g)	Application	Ref.	Paragraph
1	Ru/γ-Al₂O₃	RuCl₃nH₂O, PVP, EG, γ-Al₂O₃	MW (225W, 7 min or 450 W 2.5 min)	1.96-2.23	109-115	hydrogenation of phenol to cyclohexanone	[134]	2.1.1
2	Pd/γ-Al₂O₃	Pd(OAc)₂, γ-Al₂O₃, EG	MW (100 °C, 5 min)	3.7-8.0	-	reduction of CMA to HCMA	[135]	2.1.2
3	Pd/PK	Pd(OAc)₂, PK, ethanol	MW (100 °C, 5 min)	4.9-11.3	11.4-12.0	reduction of CMA to HCMA	[136]	2.1.3
4	Pd/G	Pd(OAc)₂, G, SDS, 1.2 MPa	MW (100 °C, 30 min)	5.0-5.9	-	hydrogenation of isophorone	[137]	2.1.4 2.2.2
5	Cu/HMS	CuNO₃, HMS, ethanol	MW (300W, 60-100 °C, 2-5 min)	3.0-5.0	-	reduction of carbonyl compounds	[138]	2.1.6 2.2.2
6	Rh/ MWCNTs	RhTDA, MWCNTs,	MW (350 W, 1 min)	3.4 – 4.3	-	hydrogenation of arenes	[139]	2.1.6 (a) 2.2.3
7	Pd or Pt/ MW-CNTs or HB-CNF or PL-CNF	Pd or Pt salt, support, Ti(OBu)₄, 1,5-pentanediol	MW (220 °C, 5 min)	-	100-201	reduction of CMA to CMO	[140]	2.1.6 (b) 2.2.1
	Ru/CNTs	RuCl₃nH₂O, PVP, ethanol/water	MW (250W, 150 °C, 12 min)	2.7-3.3	111-152	reduction of p-CNB to p-CAN	[141]	2.1.6 (c) 2.2.4
8	Pt-X/CNTs	H₂PtCl₆nH₂O and X precursor, CNTs, EtOAc	MW (165 °C, 2 min)	3.6-5.2	-	reduction of CMA to HCMA	[142]	2.1.6 (d)
9	Pd/chitosan	Pd(OAc)₂, chitosan, ethanol	MW (100 °C, 5 min)	2.9-4.8	1.7-1.9	reduction of ethyl cinnamate	[144]	2.1.7 2.2.5
10	unsupported BiRh	Bi(OAc)₃, Rh(OAc)₂, EG	MW (240 °C, 2 min)	-	-	selective hydrogenation of 1-octyne	[145]	2.1.8 2.2.1

Table 4. Synthetic conditions and characterization of the Pd nanocolloids and Pd nanocatlysts prepared using the MW-assisted solvothermal process.

Synthetic conditions	Characterization

	Pd(OAc)$_2$ (mg)	γ-Al$_2$O$_3$ (g)	Temp./time	Pd (wt%)[d]	Average diam. (nm) (Std. dev., σ)	Binding energies Pd 3d (eV)
Pd nanocolloids	41.0	-	100 °C, 5 min[a]	16.1	3.8 (σ = 1.1)	335.4 (98%) 337.4 (2%)
	41.0[c]	-	100 °C, 5 min[a]	15.8	3.7 (σ = 1.1)	335.4 (99%) 337.3 (1%)
Pd nanocatalysts	41.8	1.03	100 °C, 5 min[a]	1.9	8.0 (σ = 3.4)	335.4 (96%) 337.2 (4%)
	44.6	1.0	100 °C, 2 min[a]	2.1	5.7 (σ = 2.0)	335.3 (88%) 337.8 (12%)
	11.7	1.06	100 °C, 5 min[a]	0.7	5.2 (σ = 1.6)	335.5 (100%)
	11.7[c]	1.06	100 °C, 5 min[a]	0.7	5.1 (σ = 1.6)	335.4 (100%)
	101.1	1.03	100 °C, 5 min[a]	4.8	7.1 (σ = 3.2)	334.48(90%) 337.4 (10%)
	45.3	1.0	190 °C, 5 min[b]	2.0	6.5 (σ = 2.9)	335.3 (90%) 337.5(10%)

[a] in ethanol (40 mL) . [b] in ethylene glycol (40 mL) c 0.26 g of PVP were added d determined by ICPS and spectrophotometrical analyses.

MW volumetric heating enables more homogeneous nucleation sites in the preparation of metal nanostructured particles, leading to narrow size distributions, which is an optimal condition in catalyst preparation.[133] Many examples of MW-assisted syntheses of solid catalysts have been reported. In this paragraph, we present those designed for selective reductions.

2.1.1 Ru/γ -Al$_2$O$_3$

Galletti *et al.* developed a simple and efficient MW-assisted process for the solvothermal preparation of ruthenium nanocatalysts;[134] a MW-assisted reduction of the ruthenium salt precursor in ethylene glycol, in the presence of PVP (poly-*N*-vinyl-2-pyrrolidone) as stabilizing agent, and eventually of γ-Al$_2$O$_3$ as support. The liquid polyol acts as a solvent for the metal precursor and as reducing agent as well as being a growth medium for metal particles.

The MW-assisted solvothermal synthesis of Ru nanocolloids and supported Ru/γ-Al$_2$O$_3$ nanocatalysts was carried out using a MW applicator in which a wave guide was placed directly in the pyrex reaction vessel. Different reagent ratios and synthetic conditions influenced the characteristics and properties of the colloidal and supported Ru catalysts.

Preliminary tests of the selective,hydrogenation of phenol to cyclohexanone in solution were carried out in a mechanically stirred Parr reactor at 160 °C under 5 MPa of hydrogen. Cyclohexanone is a very important intermediate for large-scale preparation of caprolactam, the key monomer for nylon 6. It can be produced via the oxidation of cyclohexane (a low yield process) or via the hydrogenation of phenol. The latter reaction can be performed in one- or two-step process (hydrogenation to cyclohexanol which is then dehydrogenated), however, the one step selective process would appear to be more economically advantageous. Because of its importance in industrial applications, this reaction has been deeply investigated with palladium catalysts but without focusing on the cheaper ruthenium-based systems. The performances of the MW-prepared nanocatalysts, in terms of activity and selectivity, were compared with those of a commercial Ru/γ–Al$_2$O$_3$ with larger metal particles and a much broader size distribution. All the MW-prepared nanocatalysts were more active and selective than the commercial Ru/ γ-Al$_2$O$_3$.

2.1.2 Pd/γ-Al$_2$O$_3$

The same research group also reported a robust preparation method for Pd nanoparticles supported on γ-Al$_2$O$_3$, which were characterized by small diameters and narrow particle size distributions, using a low-boiling alcohol as solvent/reducing agent in the absence of any additional polymeric stabilizer.[135]

Such catalysts were prepared directly by the addition of γ-Al$_2$O$_3$ to a solution of palladium acetate in EtOH in the absence of any stabilizer, which is not always necessary. For nanoparticle stabilization the support itself can prevent significant aggregation. The resulting suspension underwent MW irradiation in a monomodal MW reactor. This approach to the preparation of nanostructured supported Pd catalysts can be of industrial relevance because the absence of additional polymeric stabilizers avoids some common detrimental effects on performance, such as the passivation of the catalyst and the reduction of specific surface area (Table 4). These supported nanocatalysts were screened via the selective reduction of CMA to HCMA, a conventional test reaction of relevant industrial and pharmacological interest (see Scheme 1).

All the catalysts showed good catalytic performances (both activity and selectivity), reaching from high to complete substrate conversions and excellent HCMA selectivity of up to 97%.

2.1.3 Pd/polyketone (Pd/PK)

New supports for Pd nanoparticles have recently been reported.[136] For the first time, the use of polyketone (poly-3-oxotrimethylene, PK), obtained by perfectly alternating CO–ethene copolymerization catalyzed by Pd(II)-diphosphine complexes has been reported. These PKs are characterized by a useful combination of mechanical, high temperature and chemical resistance and they proved to be useful candidates as support and stabilizing agents in the preparation of Pd nanoparticles. This statement has been verified by adopting three different synthetic protocols. The MW-assisted procedure was similar to those reported in previous references by the same author.[134,135]

MW heating (100 °C, 5 min) of a suspension of Pd(OAc)$_2$ and PK in ethanol gave a catalyst containing 0.6-1.0 wt% of Pd, characterized by a good average diameter (4.9-11.3 nm, σ = 1.8-4.4), BET (11.4-12.0 m^2/g) and Pd 3d$_{5/2}$ XPS binding energies (335.6 (98-99%) 337.6 (1-2%)).

These Pd/PK catalysts were screened in the selective reduction of CMA to HCMA. (See Scheme 1) Pd/PK catalysts prepared under MW showed 77-80% selectivity for HCMA at full conversionAlthough other catalysts prepared without MW irradiation showed higher selectivity, up to 80-88%, MW afforded interesting morphological features and promising catalytic performance while allowing for convenient recycling in this type of reduction. The main advantage of the MW protocol was a shorter preparation time. In addition, this methodology allows the use of milder reducing agents in comparison with the traditionally used ones such as H$_2$ and BH$_4^-$. This was further evidence that MW synthesis offers a simple, convenient, rapid and reproducible preparation route to Pd catalysts starting from commercially available Pd(II) precursors.

2.1.4 Pd/graphene (Pd/G)

The synthesis of graphene-supported Pd nanoparticles has recently been reported (Pd/G NPs). Graphene has a huge open *p*-electron system with a unique electronic structure, suitable for many applications.[137] It can be used as a catalyst or as an advantageous carrier for the catalytically active components of oxidation, reduction and carbon-carbon coupling reactions. Because of its good MW-adsorbing properties (hot surface), it can be applied in low bulk temperature selective reductions, leading to superior catalytic performance as compared to its conventional counterparts. The synthesis of the catalyst started from graphene (obtained from graphite by conventional procedure), that was mixed with palladium acetate and a sodium dodecyl sulfate solution, sonicated and finally reduced under 1.2 MPa hydrogen at 100 °C for 30 min in a pressure-resistant monomodal MW apparatus. The obtained Pd/G NPs were tested in the MW-assisted hydrogenation of isophorone, a reaction of industrial interest in the production of dihydroisophorone (DHIPO), a solvent used for vinyl resins, varnishes, lacquers, paints and other applications (see Section 2.2.2).

2.1.5 Cu/mesoporous silica (Cu/HMS)

Luque *et al.* studied reduction of carbonyl compounds (see Section 2.2.2) by employing low-loaded copper nanoparticles supported on mesoporous silica as catalysts. The catalyst was prepared according to an efficient, cheap and environmentally friendly MW-assisted protocol.[138] In essence, a solution of copper nitrate in ethanol and an appropriate amount of hexagonal mesoporous silica (HMS) were irradiated in a MW reactor for 2–5 min at 300W (60–100 °C, temperature reached) to give supported Cu nanoparticles. SEM micrographs showed that the mesoporous materials were composed of aggregates with spheroidal particles in spike-like aggregates. The particle morphology did not significantly change with Cu incorporation and, in any case, all hexagonal mesoporous silica particles maintained their spherical shape and nanoporous structure.

The effect of MW irradiation is clear. Rapid heating of reaction mixtures, especially those containing polar solvents (e.g. ethanol, water), leads to the rapid and almost simultaneous precipitation of the metal solution of the precursor which in turn renders materials with small particle sizes and narrow size distributions at very short reaction times (less than 3 min). In addition, the solvent (EtOH) facilitates the reduction of the metal in solution to elemental metal, offering better control of particle size and morphology. The porous silica support effectively prevented the coalescence of such copper/copper oxide nanocrystals thus maintaining narrow nanoparticle sizes (<5 nm).

2.1.6 Carbon nanomaterials
The use of carbon nanotubes (CNTs) as a support in heterogeneous catalysis has garnered much attention, due to their peculiar interaction with metals. Metal nanoclusters adsorbed both inside and outside CNTs usually exhibit very high activity and excellent selectivity. These advantages arise from their high mechanical strength, excellent thermal properties, absence of microporosity and absence of diffusion and material mass-transfer limitations. In addition, the metal–support interactions can generate electronic perturbations on metal particles, thus inducing a peculiar structure or a modification in the electron density in metal clusters, which can positively affect the catalyst properties.

(a) Rh/Multi-Wall CNTs

Kakade et al. reported a rapid and simple *ex situ* MW treatment for the synthesis of a Rh/multi-walled carbon nanotube (Rh/MWCNTs) hybrid material for the catalytic hydrogenation of various arenes that show enhanced turnover frequencies (TOF) over conventional catalysts.[139] Rh/MWCNTs catalysts were prepared from rhodium nanoclusters stabilized by tridecylamine (RhTDA). Tridecylamine-capped rhodium nanoparticles were directly mixed with MWCNTs (which were previously treated with acid in MW) and heated under MW for 1 min (50% of 700 W). Strong rhodium nanoparticles adsorption (3.4 – 4.3 nm; 1% w:w) on the nanotube surface, with more active sites for catalytic hydrogenation, was confirmed by TEM analysis (See Section 2.2.3 for arene hydrogenation).

(b) Pd or Pt/MWCNTs or herringbone-type carbon nanofibres (HB-CNF) or platelet-type carbon nanofibres (PL-CNF)

In recent literature, there are many other examples of functionalisation of many different carbon nanomaterials, especially MWCNTs as well as herringbone-type carbon nanofibres (HB-CNF) and platelet-type carbon nanofibres (PL-CNF). Jung *et al.* [140] synthesised carbon nanomaterials and loaded them with the active metal (platinum or palladium) by using selected functionalisation techniques. Conventional loading techniques, such as wet impregnation (WI), ion adsorption (IA), homogeneous deposition precipitation (HDP) as well as a new method, the colloidal MW process (CMP), were all applied. The latter is a MW-assisted method of preparation, which allows metal nanoparticles to be introduced onto the carbon surface without chemically modifying the carbon supports. This can be done thanks to MW heating which creates physical forces that help the binding between metal and nanomaterials. This method provides catalysts with a high metal dispersion and therefore a high efficiency in terms of activated catalyst surface. The authors studied and compared the different methods of catalyst preparation as well as the use of different supports. A special suspension of support media, metal sources and stabilizer.
After MW heating, the suspension is filtered, and dried. Finally, pyrolysis in N_2 and treatment with 10% H_2 in N_2 at 400 °C was accomplished in order to transform the catalyst to its reduced state. The samples were stored under exposure to air at room temperature and atmospheric pressure.

The liquid-phase reduction of CMA was chosen as one of the test reactions. (see Scheme 1).The aim of the investigation was to produce the intermediate product CMO, with high selectivity. The CMP-loaded catalyst showed the best catalyst performance with regards activity and selectivity as compared to the catalysts prepared using other techniques such as wet impregnation (WI), homogeneous deposition precipitation (HDP) and ion adsorption (IA) (0.95% activity and 70% selectivity towards CMO for CMP, 0.14-0.19% activity and 10-18% selectivity for other techniques).
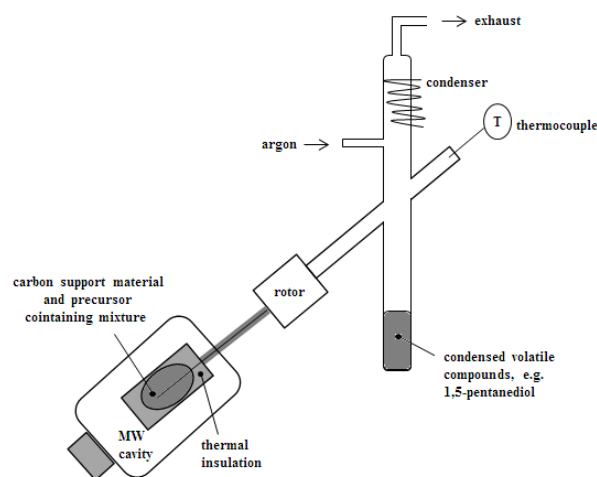These catalysts were tested also in the selective hydrogenation of 1-octyne (see Section 2.2.1).

Fig. 1 Rotating MW system [140]

(c) Ru/CNTs

Carbon nanotubes (CNTs) have been used for the preparation of supported ruthenium nanoparticles using a low boiling alcohol or an ethanol/water mixture as a solvent/reducing agent under MW irradiation.[141] Very few attempts to synthesise ruthenium nanocolloids using low boiling point alcohol and/or to prepare ruthenium nanoparticles supported on CNTs have been reported. The MW-assisted synthesis of Ru nanoparticles was performed in a monomodal MW reactor starting from $RuCl_3 \cdot 3H_2O$ and using PVP as stabilizer. For the *in situ* preparation of the supported catalysts, the desired support was directly added to the reaction vessel.

These supported ruthenium nanoparticles were characterized by small average diameters and narrow particle size distributions, even when synthesized in the absence of any additional stabilizing agents, and also appear to be very promising systems for other catalytic applications. Best synthetic conditions were 250 W, 150 °C, 1.2 MPa of nitrogen, 12 min, starting from a suspension of Ru salt and PVP in isopropanol for Ru nanocolloids. The best choice for the support was CNTs (HNO_3) in isopropanol or in H_2O/EtOH 80:20.

(d) Pt-X/CNTs

MWCNTs were used as a support for platinum-based bimetallic catalysts by Yang *et al.*[142]. These bimetallic catalysts were prepared via a facile MW-assisted polyol reduction method (MAPR) and tested in the selective reduction of CMA. The CNTs were treated with concentrated and diluted nitric acids to remove the amorphous carbonaceous and metallic impurities and to oxidize the purified CNTs to create abundant surface functional groups, which facilitated the uniform deposition of metal precursors. Pt and transition metal precursors were deposited onto functionalized CNTs and were then irradiated with MW. These bimetallic catalysts outperformed the catalysts prepared by the conventional impregnation method. CNTs surface properties, solvent selection and transition metal promoter were identified as being of great significance in tuning the catalytic performance. The best catalytic results were obtained on the Fe- and Co-modified Pt catalysts in the presence of ethyl acetate, as the

solvent, after removing the oxygen-containing groups from CNTs surfaces.

Wang, Yang *et al.*[143] prepared Pt nanoparticles supported on carbon nanotubes decorated with Fe oxides, which dramatically improve catalytic performance, due to the highly active sites formed at the interface of two metals. Fe oxides were deposited on preformed Pt nanoparticles by using a MW assisted polyol reduction method. The facile synthesis was performed in the liquid phase at 165 °C, which prevents the growth of large Pt nanoparticles and precludes the formation of a Pt–Fe alloy. Pt precursors were deposited onto functionalized CNTs by immersion of the carbon nanotubes in an aqueous solution of $H_2PtCl_6 \cdot 6H_2O$ and then drying it in a vacuum. Pt–CNTs composites were suspended in ethylene glycol, sonicated to afford a homogenous suspension and MW irradiated for few minutes to afford Pt/CNTs catalysts. Fe promoted Pt/CNTs catalysts were prepared by 4 methods. The first one was a co-impregnation method, similar to the preparation of monometallic Pt/CNTs. For the other 3 methods, Pt–Fe catalysts were synthesized via the modification of pre-synthesized Pt/CNTs. Supported Pt nanoparticles decorated with very fine Fe oxides nano-islands prepared by this two-step MW assisted method displayed improved catalytic properties in the selective reduction of CMA.

2.1.7 Pd/chitosan

Biopolymers and, in particular, polysaccharides are emerging as green and sustainable supports in heterogeneous catalysis. Among them chitosan has been investigated,[144] because of its availability, thermal stability (up to 150 °C), insolubility in the most common organic solvents and in pure water (not acidic water). Furthermore, it has high sorption capacity and the possibility of stabilizing most noble metals anions, such as Pt and Pd, thanks to the amine groups present in the natural support which are able to link the catalytic centers. The Pd/chitosan catalyst was obtained via the MW-assisted reduction of $Pd(OAc)_2$ in the presence of ethanol, which acted as both solvent and reducing agent (100 °C, 5 min). The procedure had been adapted from previously reported works of this group [118,119] The green support chitosan acts as both Pd dispersing agent and stabilizing agent. This catalyst was tested in the selective reduction of ethyl cinnamate to hydroethylcinnamate under both traditional heating and MW irradiation. Results will be discussed in the paragraph on MW-assisted selective hydrogenation. (see Section 2.2.5).

2.1.8 Unsupported catalysts: BiRh (intermetallic compound) nanoparticles

The synthesis of unsupported and nanoparticulate intermetallic compounds is beneficial, especially in catalysis, as it allows intrinsic catalytic properties to be studied without the influence of support based factors, such as strong or reactive metal−support interactions. Highly uniform and well-crystallized nanoparticles of the intermetallic compound BiRh were obtained by Ambrüster *et. al.* via synthesis at 240 °C using the MW-assisted polyol process.[145] In this time- and energy-efficient reaction, the polyol acts as solvent, reducing agent, and surfactant, while the MW radiation leads to fast and homogeneous nucleation and crystal growth. After a detailed characterization the catalytic properties of the unsupported BiRh nanoparticles were evaluated in the semi-hydrogenation of acetylene (see Section 2.2.1).

2.2 Microwave-assisted selective reductions.

The degree to which electromagnetic energy is converted into heat in a reaction medium is dependent, in practical terms, on the local strength of the electromagnetic field and on the permittivity and the permeability of the reacting mixture (solvent, reactants, reagents and solid catalyst). This practically means that both the nature of the chemicals and the geometry of the MW reactor affect heat generation in the reaction medium. It is usually accepted that a *suscepting* material is a solid or a liquid which heats up rapidly when irradiated by MW thanks to a strong interaction with the electrical or magnetic field. The addition of such a material, which is able to absorb MW energy leading to a faster heating cycle. MW heating rapidly leads to strong activation and reaction acceleration, which can negatively affect the selectivity in some cases.

2.2.1 Selective microwave-assisted hydrogenation of alkynes.

As reported in the Section 2.1.6 (b), Jung *et al.* [140] synthesized carbon nanomaterials loaded with the active metal (platinum or palladium) using selected functionalisation techniques that included MW irradiation. The selective hydrogenation of 1-octyne was investigated using palladium catalysts. The catalyst performance was assessed on the base of activity, selectivity and stability. The selective hydrogenation of 1-octyne to 1-octene was successfully realized using the two carbon nanofibre catalysts (Pd/HB-CNF - herringbone-type - and Pd/PL-CNF - platelet-type), (Table 5) which showed similar behaviour. The Pd/activated charcoal material generated side products (mainly 2- and 4-octene) most extensively with a selectivity of 37% at a conversion of 97%. The Lindlar catalyst, in contrast, showed lowest by-product formation with only 4% formation at the same conversion degree. As regards the nanofibre catalysts, an overall higher amount of side products was found in the Pd/herringbone material (14% compared to 6.3%). The selective hydrogenation to 1-octene gave modest results with the Pd/activated charcoal catalyst (20% with 97% conversion). By contrast, all other catalysts feature more promising properties. Thus, the highest selectivity values towards the desired semi-product 1-octene

Table 5. Activity and selectivity in the semi-hydrogenation of 1-octyne: comparison between Pd catalysts prepared by colloidal MW process (CMP) and commercial ones.

Catalyst	Activity [a,b] (mol/kgPdS)	Selectivity [a,d] (%)		
		$S_{1-octene}$	$S_{n-octane}$	S_{others}[c]
Pd/HB-CNF (CMP)	5.1	68.5	17.5	14.0
Pd/PL-CNF (CMP)	4.8	81.9	11.8	6.3
Lindlar catalysts (by Fluka)	5.7	88.6	7.4	4.0
Pd/activated charcoal (by Fluka)	11.9	21.0	42.0	37.0

[a] reaction conditions: 294 K, p = 0.15 MPa H_2, $m_{cat,tot}$ = 0.01 g, $c_{cat,tot}$ = 1.7 x 10^{-4} g/cm^3, $c_{0\ 1-octyne}$ = 56.2 mol/m^3. Solvent: n-heptane. [b] Initial reaction rate [c] towards by-products (mainly 2- and 4-octene) [d] selectivity at conversion of 97%

were achieved by the Lindlar catalyst and the Pt/platelet material (yield greater than 80%) while the Pt/herringbone catalyst showed a selectivity of almost 70%.

However, good selectivity and activity values were reached, particularly by the Pd/PL-material, that compare well to the

industrially established Lindlar catalyst. Long term experiments resulted in substantially higher long-term fibre material stability (Pd/PL-CNF) compared to the Lindlar catalyst. The Lindlar catalyst's faster deactivation was probably due to the presence of the poison used for selectivity enhancement.

This study shows the potential of carbon nanomaterials in the selective heterogeneous hydrogenation of alkynes.

Ambrüster et. al.[145] investigated the selective hydrogenation of acetylene, which is an important step in the industrial production of polyethylene. Traces of acetylene in the ethylene feed have to be removed since they poison the subsequent polymerization catalyst. Adsorption or catalytic conversion to ethylene are the two possible ways to remove acetylene, though only the latter is applied industrially. Highly selective catalysts are necessary to avoid ethylene loss by conversion to ethane. After a detailed characterization, the catalytic properties of the MW-prepared unsupported BiRh nanoparticles were evaluated in the semi-hydrogenation (see Section 2.1.8 for preparation).

The nanostructured BiRh sample exhibits excellent selectivity toward ethylene (88%) at a conversion of 93%. The material shows only slight deactivation during long-term acetylene hydrogenation when compared to Pd/Al_2O_3.

2.2.2 MW-assisted reduction of carbonyl compounds.

Pd/graphene (Pd/G) catalysts (see Section 2.1.4 for preparation) reported by Yang and Ma[137] have been tested in the MW-assisted selective reduction at low temperatures of isophorone, a functionalized cyclohexene derivative of commercial interest in the fine chemicals industry. Because of the similar boiling points of dihydroisophorone (DHIPO) and a by-product, high selectivity is a crucial to avoid the complicated and time-consuming product separation and purification. The high activity and high selectivity is rarely reported together. (Scheme 7)

Concerning this topic, Poliakoff *et. al.* [146] reported a method that combines supercritical fluids and continuous flow reactors. They were able to hydrogenate isophorone (at flow rates up to 2.0 mL/min at 120 bar in scCO_2 (0.75 L/min) over the 5% Pd APII Deloxan catalyst) achieving quantitative conversion with high selectivity.

However, the MW-assisted reduction of isophorone (0.5 mmol) by using Pd/G catalysts gave excellent catalytic behavior at 60 °C and 1.2 MPa hydrogen pressure in water, with a selectivity at 95%, and a TOF over 150,000/h, clearly indicating that the Pd/G catalyst is a very stable catalyst for the MW-assisted reduction.
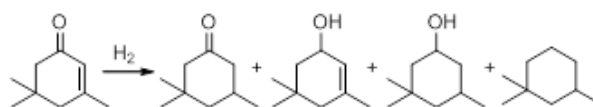

Scheme 7. The reaction of reduction of isophorone [137].

Pd/C, Pd/graphite (Pd/Grp) and Pd/SiO_2 were also tested for comparison. They exhibited activity in the selective reduction of isophorone. However, the concomitant good activity and selectivity under MW irradiation conditions was only achieved using the Pd/G nanocomposite catalyst. Both graphene and graphite possesses a giant π-system, which may promote reactant/catalysts interaction (especially for reactants with a π-system) at the same time as adsorbing MW irradiation. Indeed, Pd/Grp is much better than Pd/C and Pd/SiO_2. However, Pd/Grp

and Pd/G show different behaviour in terms of reaction performance. A possible explanation is that, as the chemically converted graphene was prepared from the reduction of graphene oxide, the edge was decorated with carboxyl groups and other oxygen-containing groups which make the catalyst well dispersed in the multi-phase reaction mixture (with water as solvent, isophorone as the organic phase and the catalyst as the solid phase). Most probably, the reaction occurred at the interfaces of the complicated reaction mixture, while the catalyst being well dispersed between the oil/water phases makes the adsorption/reaction very efficient.

The application scope of this catalytic system was explored using a variety of α, β-unsaturated ketones under similar reaction conditions. (see Table 6) The Pd/G catalyst exhibited good activity (83.7-99.0%

Table 6. MW-assisted reduction of α,β-unsaturated ketones by using Pd/G catalysts.

Substrate[a]	Conversion (%)	Ketone selectivity (%)	TOF [b]
	98.0	93.8	52 285
	97.1	99.6	51 751
	83.7	98.6	44 282
	99.1	99.6	52 818
	>99.0	<98.7	52 818

[a] 1.2 MPa H$_2$, MW 333 K, 0.5 mL H$_2$O, 2 mg 3.2% Pd/G. [b] the metal dispersion was 18.8%.

Another example of the efficient reduction of carbonyl compounds under MW irradiation was reported by Luque *et al.*[138] Cu/HMS materials prepared in MW (see Section 2.1.5) were tested as catalysts in the reduction of carbonyl compounds under MW irradiation (see Table 7)

Cu/HMS materials were found to be highly active, selective, stable and reusable in the reduction of substituted aromatic ketones and aldehydes, providing quantitative conversions starting materials within 5–10 min under mild reaction conditions with complete selectivity for the alcohols. Furthermore, the protocol is extremely attractive from the green chemistry standpoint and can be considered interesting for both industrial and academic applications.

2.2.3 Microwave-assisted hydrogenation of arenes.

Kakade et al.[139] reported the highly selective catalytic hydrogenation of arenes using rhodium nanoparticles supported on multi-walled CNTs (see part 2.1.6 (a) for preparation). The hydrogenation of arenes is a crucial step in the preparation of a wide variety of organic compounds of commercial interest. This selectivity is traditionally achieved by heterogeneous catalysis with Rh/Al$_2$O$_3$ under harsh reaction conditions. At the same time, a great deal of effort has been invested in exploring the catalytic activity of metal nanoparticles anchored on CNTs. In this work, the authors showed the activity and selectivity of Rh/MWCNTs in arene hydrogenation. In a typical experiment, a heterogeneous hydrogenation was carried out using toluene as the test substrate. A substrate to catalyst (Rh content) molar ratio of 10000:1 was

used in hexane at 40 °C and at 20 bar of H$_2$. Results are reported in Table 8. Interestingly, these materials were easily recovered by simple filtration with a considerable degree of recyclability.

2.2.4 Reduction of p-chloronitrobenzene.

Galletti *et al.*[141] have prepared Ru/CNTs catalysts (see Section 2.1.6 (c)). These systems were used to investigate the selective reduction of *p*-chloronitrobenzene (*p*-CNB) to *p*-chloroaniline (*p*-CAN). (Scheme 8)
All the catalysts gave selective nitro group reduction in *p*-CNB and the C-Cl bond was preserved. The complete conversion of substrate and selectivity to the target product were obtained under mild reaction conditions (60 °C and 4 MPa of H$_2$).
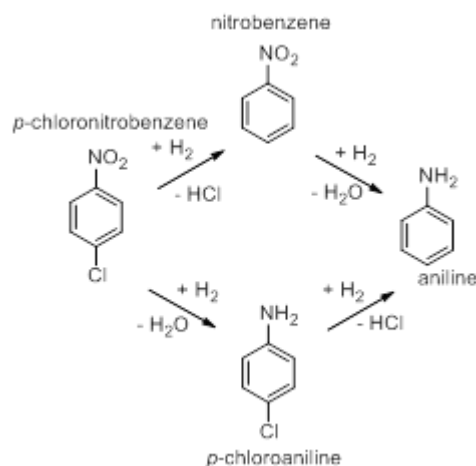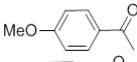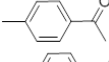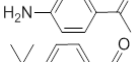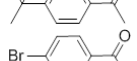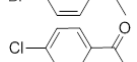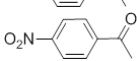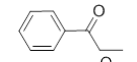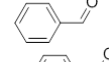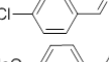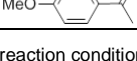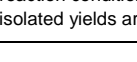

Scheme 8. The reduction pathways of *p*-chloronitrobenzene to aniline [141]

2.2.5 Reduction of ethyl cinnamate and other α,β-unsaturated carbonyl compounds.

A Pd/chitosan catalyst[144] was tested in the selective reduction of ethyl cinnamate to ethyl hydrocinnamate; a selected model reaction which holds potential interest for pharmaceutical and industrial applications. The Pd/chitosan catalyst was tested in the reduction of ethyl cinnamate (EC) to ethyl hydrocinnamate (EHC) (Scheme 9).
Reactions were carried out both in a stirred Parr autoclave and under MW irradiation, while maintaining the same reaction conditions (50 °C, 30 min, hydrogen pressure of 1 MPa) to compare results. The catalytic performance was excellent, giving full EC conversion and selectivity to EHC after 30 min, in both cases. It is remarkable that the MW-assisted reaction showed the highest reaction rate, even better than the same reaction in an autoclave at 100 °C. (see Fig. 2). Furthermore, a one pot fully MW-assisted process consisting in the synthesis of the Pd/chitosan catalyst, starting from Pd(OAc)$_2$ and chitosan in EtOH/H$_2$O, and its direct use in the reduction of ethyl cinnamate without its prior isolation and purification was carried out. No significant differences were found in the catalytic behaviour of the two-step MW and one pot MW procedures using the same amount of palladium. This approach is very promising for the direct production of hydrogenated compounds from the catalytic precursors without the catalyst's isolation and purification.

Table 7. Catalytic activity of Cu-HMS-1 in the MW-assisted reduction of aromatic carbonyl compounds[a].

Substrate[a]	Time (min)	Conversion[b] (%)	Benzylic alcohol selectivity (%)
MeO—⬡—C(O)CH₃	10	>99 (92)	>99
—⬡—C(O)CH₃	10	95 (89)	>99
H₂N—⬡—C(O)CH₃	10	92 (90)	>99
(CH₃)₃C—⬡—C(O)CH₃	15	96 (88)	>99
Br—⬡—C(O)CH₃	15	>99 (93)	>99
Cl—⬡—C(O)CH₃	15	>99 (93)	>99
O₂N—⬡—C(O)CH₃	15	90 (84)	>99
⬡—C(O)CH₂CH₃	15	94 (89)	>99
⬡—CHO	20	>99 (96)	>99
Cl—⬡—CHO	15	88 (80)	>99
MeO—⬡—C(O)CH₃	10	82	>99

[a] reaction conditions: 1 mmol substrate, 2 mL 2-propanol with NaOH (0.1 M), 0.005 g catalyst, MW 300 W, 120-130 °C
[b] isolated yields are given in brackets [c] K₂CO₃ was used replacing NaOH [d] reused recovered catalyst after 5 uses

Table 8. Efficiency and selectivity of the Rh/MW-CNTs hybrid material for arene hydrogenation[a].

Substrate	Product	Time (h)	Conversion (%)	Selectivity (%)	TON	TOF
m-xylene	1,3-dimethylcyclohexane	4	99	82 (cis) 18 (trans)	9900	2475
p-xylene	1,4-dimethylcyclohexane	4	99	72 (cis) 28 (trans)	9900	2475
o-xylene	1,2-dimethylcyclohexane	4	96	91 (cis) 9 (trans)	9600	2400
p-cresol	4-methylcyclohexanol	4	87	97 (cis) 3 (trans)	8700	2175

[a] reaction conditions: 5 mmol of substrate, 5 mg of catalyst (0.0005 mmol), 50 mL of hexane, 40 °C, 20 bar of H₂

.

As reported in Section 2.1.7, several α,β-unsaturated carbonyl compounds such as cyclohex-2-enone, benzalacetophenone, 1,2-diphenylacetylene and *N*-benzylideneaniline were successfully hydrogenated in ethanol under mild MW irradiation conditions (50 °C, 6 bar) in a multimode reactor, while maintaining a pH of around 2.[87] Reaction parameters like temperature, hydrogen pressure and the solvent were varied. It was shown that the reduction of the catalyst is crucial for catalytic activity. The catalyst was reused ten times in the reduction of cyclohex-2-enone, without showing any observable loss in immobilized metal content. The polymeric support material did not show any decomposition.
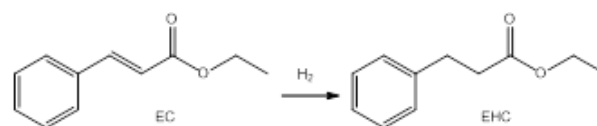
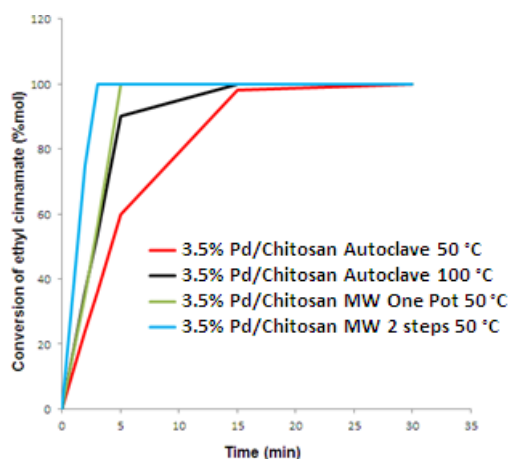Scheme 9. Reduction reaction of ethyl cinnamate (EC) to ethyl hydrocinnamate (EHC) [144].

Fig. 2 Conversion of ethyl cinnamate (mol%) vs. time curves [144]
.

Summary and Outlook.

The use of MW and/or US for the preparation of catalysts and selective reductions with H_2 can significantly reduce the limitations in terms of yields and long reaction times observed under conventional conditions. Especially in the preparation of catalysts, the use of US and MW results in more uniform particle size distribution with less agglomeration and better dispersion. Catalysts are generally significantly more active and can also be more selective. The last generation of dedicated microwave reactors (see graphical abstract figure) especially designed for extreme reaction conditions, guarantee a maximum of user safety when working at high temperatures and pressure. Their versatility enables synthetic processes from milligram to multigrams scale with a fast screening of best reaction conditions. Analogously ultrasonic reactors working under gas pressure are an irreplaceable tool for this type of investigation.

In the future, supplies of energy and platinum group metals will become scarcer and more expensive, therefore the use of more active catalysts and more focused, rapid, localized heating will be critical for the production of chemicals. As such, it is clear that MW- and US-promoted transformations will continue to act as enabling technologies that will spur further developments both on a laboratory and an industrial scale. In addition, we expect the combination of US and MW with flow chemistry to bring additional benefits in terms of production capacity, activity, selectivity and reduced energy usage.

[1] F. Zaera, *Catal. Lett.* **2012**, *142*, 501-516.
[2] G. Cravotto, L. Orio, E. C. Gaudino, K. Martina, D. Tavor, A. Wolfson, *ChemSusChem* **2011**, *4*, 1130-1134.
[3] G. Kaupp, *CrystEngComm* **2006**, *8*, 794-804.
[4] R. Ciriminna, M. Pagliaro, *Org. Process Res. Dev.* **2013**, *17*, 1479-1484.
[5] M. Cargnello, P. Fornasiero, R. J. Gorte, *ChemPhysChem* **2013**, *14*, 3869-3877.
[6] Y. Yu, Z. Hou, *Curr. Org. Chem.* **2013**, *17*, 336-347.
[7] G. Cravotto, S. Tagliapietra, M. Caporaso, D. Garella, E. Borretto, A. Di Stilo, *Chem. Het. Comp.* **2013**, *49*, 811-826.
[8] G. Cravotto, W. Bonrath, S. Tagliapietra, C. Speranza, E. C. Gaudino, A. Barge, *Chem. Eng. Proc.* **2010**, *49*, 930-935.
[9] V. Hessel, G. Cravotto, P. Fitzpatrick, B. S. Patil, J. Lang, W. Bonrath, *Chem. Eng. Proc.* **2013**, *71*, 19-30.
[10] D. H. Shin, B. H. Han, *Bull. Korean Chem. Soc.* **1985**, *6*, 247-248.
[11] T. J. Mason, J. P. Lorimer, *Sonochemistry: Theory, Applications and Uses of Ultrasound in Chemistry*; Ellis Horwood Ltd.: Chichester, 1988, 91, 96.
[12] K. S. Suslick, S. E. Skrabalak, *Sonocatalysis* in *Handbook of Heterogeneous Catalysis*; G. Ertl, H. Knozinger, F. Schuth, J. Weitkamp, Eds.; Wiley-VCH, 2008; Vol. 4, 2007.
[13] A. Barge, S. Tagliapietra, L. Tei, P. Cintas, G. Cravotto, *Curr. Org. Chem.* **2008**, *12*, 1588-1612.
[14] W. Bonrath, R. A. P. Schmidt, *Ultrasound in Synthetic Organic Chemistry* in *Advances in Organic Synthesis*; Atta-ur-Rahman, Ed.; Bentham Science Publishers., 2005; Vol. 1, 81-117.
[15] U. R. Pillai, E. Sahle-Demessie, R. S. Varma, *J. Mater. Chem.* **2002**, *12*, 3199-3207.
[16] S. Puri, B. Kaur, A. Parmar, H. Kumar, *Curr. Org. Chem.* **2013**, *17*, 1790-1828.
[17] B. Toukoniitty, J. P. Mikkola, D. Y. Murzin, T. Salmi, *Appl. Catal. A. Gen.* **2005**, *279*, 1-22.
[18] P. Cintas, J. L. Luche, *Green Chem.* **1999**, *1*, 115-125.
[19] Y. G. Adewuyi, *Ind. Eng. Chem. Res.* **2001**, *40*, 4681-4715.
[20] J.-L. Luche, C. Bianchi, *Synthetic organic sonochemistry*; Springer, 1998, 185-188, 241-253.
[21] K. S. Suslick, *Science* **1990**, *247*, 1439-1445.
[22] K. S. Suslick, S. B. Choe, A. A. Cichowlas, M. W. Grinstaff, *Nature* **1991**, *353*, 414-416.
[23] N. A. Dhas, A. Gedanken, *Chem. Mat.* **1997**, *9*, 3144-3154.
[24] T. Prozorov, R. Prozorov, K. S. Suslick, *J. Am. Chem. Soc.* **2004**, *126*, 13890-13891.
[25] Y. Pei, G. Zhou, N. Luan, B. Zong, M. Qiao, F. F. Tao, *Chem. Soc. Rev.* **2012**, *41*, 8140-8162.
[26] L. A. Crum, *Ultrason. Sonochem.* **1995**, *2*, S147-S152.
[27] B. Török, K. Balázsik, K. Felföldi, M. Bartók, *Ultrason. Sonochem.* **2001**, *8*, 191-200.
[28] A. Kulkarni, B. Török, *Curr. Org. Synth.* **2011**, *8*, 187-207.
[29] M. Atobe, M. Okamoto, T. Fuchigami, J.-E. Park, *Ultrason. Sonochem.* **2010**, *17*, 26-29.
[30] D. Adam, *Nature* **2003**, *421*, 571-572.
[31] R. Gedye, F. Smith, K. Westaway, H. Ali, L. Baldisera, L. Laberge, J. Rousell, *Tetrahedron Lett.* **1986**, *27*, 279-282.
[32] R. J. Giguere, T. L. Bray, S. M. Duncan, G. Majetich, *Tetrahedron Lett.* **1986**, *27*, 4945-4948.
[33] C. O. Kappe, *Angew. Chem. Int. Ed.* **2004**, *43*, 6250-6284.
[34] D. M. P. Mingos, D. R. Baghurst, *Chem. Soc. Rev.* **1991**, *20*, 1-47.
[35] S. Caddick, *Tetrahedron* **1995**, *51*, 10403-10432.
[36] T. S. Ahmadi, Z. L. Wang, T. C. Green, A. Henglein, M. A. ElSayed, *Science* **1996**, *272*, 1924-1926.
[37] W. Y. Yu, W. X. Tu, H. F. Liu, *Langmuir* **1999**, *15*, 6-9.

[38] W. X. Tu, H. F. Lin, *Chem. Mat.* **2000**, *12*, 564-567.
[39] W. X. Chen, J. Y. Lee, Z. L. Liu, *Chem. Commun.* **2002**, 2588-2589.
[40] L. H. Thompson, L. K. Doraiswamy, *Ind. Eng. Chem. Res.* **1999**, *38*, 1215-1249.
[41] B. Toukoniitty, E. Toukoniitty, P. Maki-Arvela, J. P. Mikkola, T. Salmi, D. Y. Murzin, P. J. Kooyman, *Ultrason. Sonochem.* **2006**, *13*, 68-75.
[42] I. Kun, B. Török, K. Felföldi, M. Bartók, *Appl. Catal. A. Gen.* **2000**, *203*, 71-79.
[43] A. Tai, T. Kikukawa, T. Sugimura, Y. Inoue, T. Osawa, S. Fujii, *Journal of the Chemical Society, Chemical Communications* **1991**, 795-796.
[44] J. Lindley, *Ultrasonics* **1992**, *30*, 163-167.
[45] Y.-F. Han, H.-M. Wang, H. Cheng, J.-F. Deng, *Chem. Commun.* **1999**, 521-522.
[46] X. Tang, S. Liu, Y. Wang, W. Huang, E. Sominski, O. Palchik, Y. Koltypin, A. Gedanken, *Chem. Commun.* **2000**, 2119-2120.
[47] U. R. Pillai, E. Sahle-Demessie, R. S. Varma, *Appl. Catal. A. Gen.* **2003**, *252*, 1-8.
[48] C. L. Bianchi, F. Martini, V. Ragaini, *Ultrason. Sonochem.* **2001**, *8*, 131-135.
[49] K. S. Suslick, D. J. Casadonte, M. L. H. Green, M. E. Thompson, *Ultrasonics* **1987**, *25*, 56-59.
[50] E. B. Flint, K. S. Suslick, *Science* **1991**, *253*, 1397-1399.

[51] D. Chu, H. Li, H. Li, *Petrochem. Technol.* **2006**, *12*, 1125-1129.
[52] K. S. Suslick, T. W. Hyeon, M. M. Fang, *Chem. Mat.* **1996**, *8*, 2172-2179.
[53] K. S. Suslick, S. J. Doktycz, *J. Am. Chem. Soc.* **1989**, *111*, 2342-2344.
[54] K. S. Suslick, T. Hyeon, M. M. Fang, A. A. Cichowlas, *Mater. Sci. Eng. A-Struct. Mater. Prop. Microstruct. Process.* **1995**, *204*, 186-192.
[55] T. H. Hyeon, M. M. Fang, K. S. Suslick, *J. Am. Chem. Soc.* **1996**, *118*, 5492-5493.
[56] M. M. Mdleleni, T. Hyeon, K. S. Suslick, *J. Am. Chem. Soc.* **1998**, *120*, 6189-6190.
[57] A. P. Newman, J. P. Lorimer, T. J. Mason, K. R. Hutt, *Ultrason. Sonochem.* **1997**, *4*, 153-156.
[58] K. Okitsu, Y. Mizukoshi, H. Bandow, Y. Maeda, T. Yamamoto, Y. Nagata, *Ultrason. Sonochem.* **1996**, *3*, S249-S251.
[59] C. Bianchi, R. Carli, S. Lanzani, D. Lorenzetti, G. Vergani, V. Ragaini, *Ultrason. Sonochem.* **1994**, *1*, S47-S49.
[60] C. L. Bianchi, E. Gotti, L. Toscano, V. Ragaini, *Ultrason. Sonochem.* **1997**, *4*, 317-320.
[61] H. Li, J. Zhang, H. Li, *Catal. Commun.* **2007**, *8*, 2212-2216.
[62] H. Li, H. Li, J. Zhang, W. Dai, M. Qiao, *J. Catal.* **2007**, *246*, 301-307.
[63] X. Chen, Z. Lou, S. Xie, M. Qiao, S. Yan, Y. Zhu, K. Fan, H. He, *Chem. Lett.* **2006**, *35*, 390-391.
[64] J. Li, T. Inui, *Appl. Catal. A. Gen.* **1996**, *139*, 87-96.
[65] J. Guo, Y. Hou, C. Yang, Y. Wang, H. He, W. Li, *Catal. Commun.* **2011**, *16*, 86-89.
[66] J. Guo, Y. Hou, C. Yang, Y. Wang, L. Wang, *Mater. Lett.* **2012**, *67*, 151-153.
[67] H. Li, Y. Wang, Q. Zhao, H. Li, *Res. Chem. Intermed.* **2009**, *35*, 779-790.

[68] Y. Wang, L. Xu, L. Xu, H. Li, H. Li, *Chin. J. Catal.* **2013**, *34*, 1027-1032.
[69] G. Bai, L. Niu, M. Qiu, F. He, X. Fan, H. Dou, X. Zhang, *Catal. Commun.* **2010**, *12*, 212-216.
[70] Y. Hou, Y. Wang, F. He, W. Mi, Z. Li, Z. Mi, W. Wu, E. Min, *Appl. Catal. A. Gen.* **2004**, *259*, 35-40.
[71] G. Bai, L. Niu, Z. Zhao, N. Li, F. Li, M. Qiu, F. He, G. Chen, Z. Ma, *J. Mol. Catal. A. Chem.* **2012**, *363-364*, 411-416.
[72] Q. Wang, H. Yang, J. Zhu, X. Chen, H. Li, *J. Shanghai Teach. Univ.* **2002**, *4*, 012.
[73] W. Li, Z. Liu, *Ind. Catal.* **2008**, *16*, 11-16.
[74] W. Huang, H. Li, B. Zhu, Y. Feng, S. Wang, S. Zhang, *Ultrason. Sonochem.* **2007**, *14*, 67-74.
[75] Y. Zeng, Q. Yang, J. Sun, B. Zhu, L. Pan, Y. Wen, Z. Zhang, *Titan. Ind. Prog.* **2007**, *24*, 42-45.
[76] G. Szollosi, B. Török, G. Szakonyi, I. Kuna, M. Bartók, *Appl. Catal. A. Gen.* **1998**, *172*, 225-232.
[77] S. J. Doktycz, K. S. Suslick, *Science* **1990**, *247*, 1067-1069.
[78] S. Wei, H. Cui, J. Wang, S. Zhuo, W. Yi, L. Wang, Z. Li, *Particuology* **2011**, *9*, 69-74.
[79] S. Xie, H. Li, H. Li, J.-F. Deng, *Appl. Catal. A. Gen.* **1999**, *189*, 45-52.
[80] M. Vilar, M. Navarro, *Electrochim. Acta* **2012**, *59*, 270-278.
[81] S. Devarakonda, J. M. Evans, A. S. Myerson, *Cryst. Growth Des.* **2003**, *3*, 741-746.
[82] X. Fu, L. Sang, S. Bai, Q. Yang, J. Wang, Y. Sun, S. Zeng, *Chin. J. Chem. Phys.* **2000**, *13*, 503-507.

[83] A. Giroir-Fendler, D. Richard, P. Gallezot, *Catal. Lett.* **1990**, *5*, 175-181.
[84] F. Delbecq, P. Sautet, *J. Catal.* **1995**, *152*, 217-236.
[85] B. Török, I. Painko, A. Molmst, M. Bartók, *J. Catal.* **1993**, *143*, 111-121.
[86] G. Cravotto, D. Garella, S. Tagliapietra, A. Stolle, S. Schüßler, S. E. Leonhardt, B. Ondruschka, *New J. Chem.* **2012**, *36*, 1304-1307.
[87] S. Schüßler, N. Blaubach, A. Stolle, G. Cravotto, B. Ondruschka, *Appl. Catal. A. Gen.* **2012**, *445-446*, 231-238.
[88] W. Bonrath, *Ultrason. Sonochem.* **2005**, *12*, 103-106.
[89] A. Barge, S. Tagliapietra, A. Binello, G. Cravotto, *Curr. Org. Chem.* **2011**, *15*, 189-203.
[90] G. Cravotto, P. Cintas, *Chem. Eur. J.* **2007**, *13*, 1902-1909.
[91] G. Cravotto, P. Cintas, *Angew. Chem.-Int. Edit.* **2007**, *46*, 5476-5478.
[92] G. Cravotto, P. Cintas, *Chem. Soc. Rev.* **2006**, *35*, 180-196.
[93] W. Bonrath, *Ultrason. Sonochem.* **2003**, *10*, 55-59.
[94] W. Bonrath, *Ultrason. Sonochem.* **2004**, *11*, 1-4.
[95] K. S. Suslick, Ed. *Sonocatalysis; Wiley*-VCH: Weinheim,, 1997; Vol. 3.
[96] G. Szollosi, I. Kun, B. Török, M. Bartók, *Ultrason. Sonochem.* **2000**, *7*, 173-176.
[97] T. J. Mason, *Chem. Soc. Rev.* **1997**, *26*, 443-451.
[98] J. P. Mikkola, B. Toukoniitty, E. Toukoniitty, J. Aumo, T. Salmi, *Ultrason. Sonochem.* **2004**, *11*, 233-239.
[99] R. S. Disselkamp, T. R. Hart, A. M. Williams, J. F. White, C. H. F. Peden, *Ultrason. Sonochem.* **2005**, *12*, 319-324.
[100] H. Li, C. J. Ma, H. X. Li, *Chin. J. Chem.* **2006**, *24*, 613-619.
[101] B. Török, K. Felföldi, G. Szakonyi, M. Bartók, *Ultrason. Sonochem.* **1997**, *4*, 301-304.

[102] K. Balázsik, B. Török, K. Felföldi, M. Bartók, Ultr*ason. Sonochem. 1999*, **5,** 1*4*9-155.

[103] K. J. Moulton, S. Koritala, E. N. Frankel., J. A*m. Oil Chem. Soc. 198*3, **60**, *1*257.

[104] B. Török, G. Szollosi, K. Balozsik, K. Felföldi, I. Kun, M. Bartók, Ultr*ason. Sonochem. 1999*, **6,** 9*7*-103.

[105] P. Cains, L. McCausland, D. Bates, T. Mason, Ultr*ason. Sonochem. 1994*, **1,** S*4*5-S46.

[106] M. G. Sulman, Russ*. Chem. Rev. 200*0, **69**, *1*65-177.

[107] P. Boudjouk, B.-H. Han, J. C*atal. 198*3, **79**, 4*8*9-492.

[108] M. K. Basu, F. F. Becker, B. K. Banik, J. C*hem. Research (S) 200*0, **40**6-407.

[109] M. K. Basu, F. F. Becker, B. K. Banik, Tetr*ahedron Lett. 200*0, **41**, *5*603-5606.

[110] D. Nagaraja, M. Pasha, Tetr*ahedron Lett. 199*9, **40**, 7*8*55-7856.

[111] S. C. Mhadgut, I. Bucsi, M. Török, B. Török, Chem. *Commun. 200*4, **98**4-985.

[112] R. S. Disselkamp, Y. H. Chin, C. H. F. Peden, J. C*atal. 200*4, **227**, *5*52-555.

[113] P. J. Wan, M. wa Muanda, J. E. Covey, J. A*m. Oil Chem. Soc. 199*2, **69**, 8*7*6-879.

[114] A. B. Gamble, J. Garner, C. P. Gordon, S. M. O'Conner, P. A. Keller, Synt*h. Commun. 200*7, **37**, *2*777-2786.

[115] B. Török, K. Balozsik, M. Török, K. Felföldi, M. Bartók, Cata*l. Lett. 200*2, **81**, *5*5-62.

[116] R. S. Disselkamp, K. M. Judd, T. R. Hart, C. H. Peden, G. J. Posakony, L. J. Bond, J. C*atal. 200*4, **22**1, *3*47-353.

[117] R. S. Disselkamp, Y.-H. Chin, C. H. Peden, Jour*nal of Catalysis 200*4, **22**7, *5*52-555.

[118] R. S. Disselkamp, K. M. Denslow, T. R. Hart, J. F. White, C. H. Peden, Appl. *Catal. A. Gen. 200*5, **28**8, *6*2-66.

[119] B. Toukoniitty, J. Kuusisto, J. P. Mikkola, T. Salmi, D. Y. Murzin, Ind. *Eng. Chem. Res. 200*5, **44**, *9*370-9375.

[120] H. Lindlar, R. Dubuis, Org. *Synth. 196*6, **89**-89.

[121] G. Sharma, B. Choudary, M. R. Sarma, K. K. Rao, J. O*rg. Chem. 198*9, **54**, *2*997-2998.

[122] R. Nishio, M. Sugiura, S. Kobayashi, Org. *Biomol. Chem. 200*6, **4,** 9*9*2-995.

[123] F. Alonso, I. Osante, M. Yus, Tetr*ahedron 200*7, **63**, *9*3-102.

[124] H. M. Sheldrake, T. W. Wallace, Tetr*ahedron Lett. 200*7, **48**, *4*407-4411.

[125] F. Studt, F. Abild-Pedersen, T. Bligaard, R. Z. Sarensen, C. H. Christensen, J. K. Narskov, Scie*nce 200*8, **32**0, *1*320-1322.

[126] D. Duraczynska, E. M. Serwicka, A. Drelinkiewicz, Z. Olejniczak, Appl. *Catal. A. Gen. 200*9, **37**1, *1*66-172.

[127] S. Nikolaev, V. Smirnov, Cata*l. Today 200*9, **147**, *S*336-S341.

[128] P. T. Witte, S. Boland, F. Kirby, R. v. Maanen, B. F. Bleeker, D. A. M. d. Winter, J. A. Post, J. W. Geus, P. H. Berben., Chem*CatChem 201*3, **5,** 5*8*2 - 587.

[129] G. Saracco, F. Arzano, La *Chimica e L'Industria 196*8, **50**, *3*14-316.

[130] P.N. Pintauro, M. P. Gil, K. Warner, G. List, W. Neff, *Ind. Eng. Chem. Res.*, **2005**, *44*, 6188-6195.

131] M. Pasha, V. Jayashankara, Ultr*ason. Sonochem. 200*5, **12**, *4*33-435.

[132] H. M. Hung, F. H. Ling, M. R. Hoffmann, Envi*ron. Sci. Technol. 200*0, **34**, *1*758-1763.

[133] P. T. Anastas, L. B. Bartlett, M. M. Kirchhoff, T. C. Williamson, Cata*l. Today 200*0, **55**, *11*-22.

[134] A. M. R. Galletti, C. Antonetti, I. Longo, G. Capannelli, A. M. Venezia, Appl. *Catal. A. Gen. 200*8, **35**0, *46*-52.

[135] A. M. R. Galletti, C. Antonetti, A. M. Venezia, G. Giambastiani, Appl. *Catal. A. Gen. 201*0, **38**6, *1*24-131.

[136] A. M. R. Galletti, L. Toniolo, C. Antonetti, C. Evangelisti, C. Forte, Appl. *Catal. A. Gen. 201*2, **44**7*-448, 4*9-59.

[137] J. Yang, D. Ma, RSC *Adv. 201*3, **3,** 1*0*131-10134.

[138] K. Yoshida, C. Gonzalez-Arellano, R. Luque, P. L. Gai, Appl. *Catal. A. Gen. 201*0, **37**9, *3*8-44.

[139] B. A. Kakade, S. Sahoo, S. B. Halligudi, V. K. Pillai, J. P*hys. Chem. C 200*8, **11**2, *1*3317-13319.

[140] A. Jung, A. Jess, T. Schubert, W. Sch 眉 tz, Appl. *Catal. A. Gen. 2009*, **362**, *9*5-105.

[141] C. Antonetti, M. Oubenali, A. M. Raspolli Galletti, P. Serp, G. Vannucci, Appl. *Catal. A. Gen. 2012*, **421**, *99*-107.

[142] Z. Guo, Y. Chen, L. Li, X. Wang, G. L. Haller, Y. Yang, J. C*atal. 2010*, **276**, *3*14-326.

[143] Z. Guo, C. Zhou, D. Shi, Y. Wang, X. Jia, J. Chang, A. Borgna, C. Wang, Y. Yang, Appl. *Catal. A. Gen. 2012*, **435**, *1*31-140.

[144] A. M. R. Galletti, C. Antonetti, M. Bertoldo, F. Piccinelli, Appl. *Catal. A. Gen. 2013*, **468**, *9*5-101.

[145] D. Köhler, M. Heise, A. I. Baranov, Y. Luo, D. Geiger, M. Ruck, M. Armbrüster, Chem. M*at. 2012, *2*4*, **1**6*3*9-1644.

[146] M. G. Hitzler, F. R. Smail, S. K. Ross, M. Poliakoff, Org Pro*cess Res Dev. 1998, *2**, 1**37-*1*46.

Entry for the Table of Contents (Please choose one layout only)

Layout 1:

REVIEW

Besides enhancing reaction rates, ultrasound and microwaves may help to drive reduction processes to highly selective pathway.

Z. Wu, E. Borretto, J. Medlock, W. Bonrath and G. Cravotto*

Page No. – Page No.

Effects of Ultrasound and Microwaves on Selective Reduction: Catalyst Preparation and Reactions